

Marquette University

e-Publications@Marquette

---

Master's Theses (2009 -)


Dissertations, Theses, and Professional  
Projects

---

## Synthesis and Characterization of Enantioenriched Deuterated and Fluorinated Small Molecules

Mitchell D. Mills  
*Marquette University*

Follow this and additional works at: [https://epublications.marquette.edu/theses\\_open](https://epublications.marquette.edu/theses_open)

 Part of the [Chemistry Commons](#)

---

### Recommended Citation

Mills, Mitchell D., "Synthesis and Characterization of Enantioenriched Deuterated and Fluorinated Small Molecules" (2022). *Master's Theses (2009 -)*. 712.  
[https://epublications.marquette.edu/theses\\_open/712](https://epublications.marquette.edu/theses_open/712)

SYNTHESIS AND CHARACTERIZATION OF ENANTIOENRICHED  
DEUTERATED AND FLUORINATED SMALL MOLECULES

by

Mitchell Mills

A Thesis submitted to the Faculty of the Graduate School,  
Marquette University,  
in Partial Fulfillment of the Requirements for  
the Degree of Master of Science

Milwaukee, Wisconsin

May 2022

ABSTRACT  
SYNTHESIS AND CHARACTERIZATION OF ENANTIOENRICHED  
DEUTERATED AND FLUORINATED SMALL MOLECULES

Mitchell Mills

Marquette University, 2022

The development of novel deuterated and fluorinated bioisosteres has significantly impacted the pharmaceutical and agricultural industry and created a growing demand for new synthetic methodology. Both deuterated and fluorinated small molecules exist at the forefront of drug discovery due to their unique ability to attenuate the pharmacokinetic properties of new and currently existing drugs. Selective, high-throughput methods for deuteration and fluorination are scarce in the literature, especially methods that introduce D or F atoms asymmetrically. Benzylic C–H bonds are oftentimes key sites for enzymatic manipulation in metabolic processes, alteration of C–H bonds to C–D or C–F bonds at the benzylic site of organic molecules affects the metabolic process, making this a key site for bioisosterism. Using state-of-the-art methods to synthesize chiral by virtue of deuterium small molecules requires significant synthetic overhead with limited methods for chiral analysis due to the similar nature of H and D. Asymmetric fluorination has been restricted to  $\alpha,\beta$ -unsaturated carbonyl compounds that can transform into metal enolates, and only two literature examples of enantioselective fluorinations of aryl alkenes. Herein, enantioselective methods for both deuteration and fluorination are described.

Regio- and enantioselective hydrodeuteration of the  $\pi$ -bond of aryl alkenes was successfully achieved using a chiral Cu–H catalyst with a protic D-source. Molecular rotational resonance (MRR) spectroscopy was utilized as a novel analytical method for determining %ee, absolute stereochemistry, and identifying isotopomers and isotopologues. This substrate scope includes various aromatic and heteroaromatic alkenes with excellent yields and high enantioselectivities. By substituting the protic D-source for Selectfluor, an electrophilic fluorinating reagent, enantioselective fluorination was also achieved. Optimization of the catalytic conditions will reveal the feasibility of achieving high enantioselectivities and yields. In this work, my contributions to both the deuteration and fluorination projects is described.

## ACKNOWLEDGMENTS

Mitchell Mills

I would like to thank my research advisor, Dr. Joseph R. Clark, for his guidance and wisdom throughout the program. Thank you to my fellow graduate students, Sam Hintzsche, Samantha Sloane, and Zoua Pa Vang for your friendship and assistance. Thank you to my committee members, Dr. Chae Yi and Dr. Dian Wang, for supporting me as a chemist. Thank you to my parents, Ron and Jane Mills, for pushing me to pursue my passions. A special thanks to my love, Nicole Nettell, for your endless compassion, I could not have done this without you.

## TABLE OF CONTENTS

ACKNOWLEDGMENTS.....	i
LIST OF TABLES.....	iii
LIST OF FIGURES.....	iv
CHAPTER	
1. CU-CATALYZED ENANTIOSELECTIVE HYDRODEUTERATION OF ALKENYL ARENES.....	1
1.1. Introduction.....	1
1.2. State-of-the-Art Methods for Installation of Deuterium into Small Organic Molecules.....	2
1.3. Chiral by Virtue of Deuterium Small Molecules.....	4
1.4. Research Objectives and Reaction Development.....	9
1.5. Chiral Analysis of Enantioenriched Chiral by Virtue of Deuterium Small Molecules using Molecular Rotational Resonance Spectroscopy.....	12
1.6. Synthesis and Chiral MRR Analysis of <i>dl</i> -Ethylbenzene.....	20
1.7. Reaction Optimization and Substrate Scope.....	23
1.8. Future Work.....	26
2. CU-CATALYZED ENANTIOSELECTIVE FLUORINATION OF ALKENYL ARENES.....	28
2.1 Introduction.....	28
2.2. History of Fluorination and State-of-the-Art Methods for Metal- Catalyzed Hydrofluorinations.....	30
2.3. Initial Results and Future Work.....	36
BIBLIOGRAPHY.....	44
METHODS AND MATERIALS.....	53

## LIST OF TABLES

<b>Table 1:</b> Optimization of Solvent and Temperature for Transfer Deuteration.....	25
---	----

## LIST OF FIGURES

<b>Figure 1:</b> Metal-Catalyzed Stereoretentive Hydrogen Isotope Exchange.....	2
<b>Figure 2:</b> Stereoselective Synthesis of Deuterated Cyclohexene Derivatives with a Tungsten Complex.....	3
<b>Figure 3:</b> State-of-the-Art Regioselective Reductive Deuteration of an Aryl Alkenes.....	4
<b>Figure 4:</b> Mosher Synthesis of <i>dl</i> -Ethylbenzene.....	5
<b>Figure 5:</b> Christoffers Synthesis and derivatization of <i>dl</i> -Ethylbenzene.....	6
<b>Figure 6:</b> Flood's Synthesis of <i>dl</i> -( <i>R</i> )-(-)-8-( $\alpha$ -deuterioethyl)quinoline.....	8
<b>Figure 7:</b> Cu-Catalyzed Transfer Deuteration of Aryl Alkynes.....	10
<b>Figure 8:</b> Proposed Mechanism for Enantioselective Cu-Catalyzed Hydrodeuteration of Aryl Alkenes.....	12
<b>Figure 9:</b> Broadband MRR Instrument and IsoMRR Instrument.....	13
<b>Figure 10:</b> Initial Study of Catalytic Regio- and Enantio- Selective Aryl Alkene Transfer Deuteration.....	15
<b>Figure 11:</b> Sample 3-D Models of Chiral Tag-Analyte Diastereomer Complexes.....	17
<b>Figure 12:</b> Formation of Homochiral and Heterochiral Diastereomer Substrate-Tag Complexes for MRR analysis.....	18
<b>Figure 13:</b> MRR Spectra of <i>dl</i> -3-Phenylpropanol with Racemic Propylene Oxide and ( <i>S</i> )-Propylene Oxide.....	19
<b>Figure 14:</b> Zoomed in Comparison of Homochiral and Heterochiral Transition Signals with ( <i>S</i> )-Propylene Oxide.....	20
<b>Figure 15:</b> Sample 3-D Models of Chiral Tag-Analyte Diastereomer Complexes.....	21
<b>Figure 16:</b> Formation of Homochiral and Heterochiral Diastereomer Substrate-Tag Complexes for MRR Analysis.....	22
<b>Figure 17:</b> Summary of MRR Chiral Analysis of <i>dl</i> -Ethylbenzene Samples.....	22

<b>Figure 18:</b> Comparison of Synthetic Routes and EE's of ( <i>S</i> )- <i>dl</i> -Ethylbenzene using MRR Analysis.....	23
<b>Figure 19:</b> Transfer Hydrodeuteration Substrate Scope.....	26
<b>Figure 20:</b> Future Substrate Scope for Transfer Hydrodeuteration Project.....	27
<b>Figure 21:</b> N-Quaternization Strategy for Improved Enantioselectivity of N-Containing Heteroaryl Alkenes.....	27
<b>Figure 22:</b> Blockbuster Organofluorine Commercial Drugs.....	30
<b>Figure 23:</b> Pioneering Work in Alkene Fluorination.....	31
<b>Figure 24:</b> Fluorinating Reagents.....	32
<b>Figure 25:</b> First Enantioselective Fluorination using a Chiral Fluorinating Reagent.....	34
<b>Figure 26:</b> Previous Work and State-of-the-Art Enantioselective Transition Metal-Catalyzed Hydrofluorination of Alkenyl Arenes.....	35
<b>Figure 27</b> Preliminary Results for Enantioselective Cu-Catalyzed Hydrofluorination...	38
<b>Figure 28:</b> Proposed Mechanism for Enantioselective Cu-Catalyzed Hydrofluorination of Aryl Alkenes.....	39
<b>Figure 29:</b> Synthesis of Selectfluor and Proposed Selectfluor Derivatives.....	42
<b>Figure 30:</b> Initial Proposed Substrate Scope for the Hydrofluorination of Alkenyl Arenes.....	43



## Chapter 1: Cu-Catalyzed Enantioselective Hydrodeuteration of Alkenyl Arenes

### 1.1 Introduction

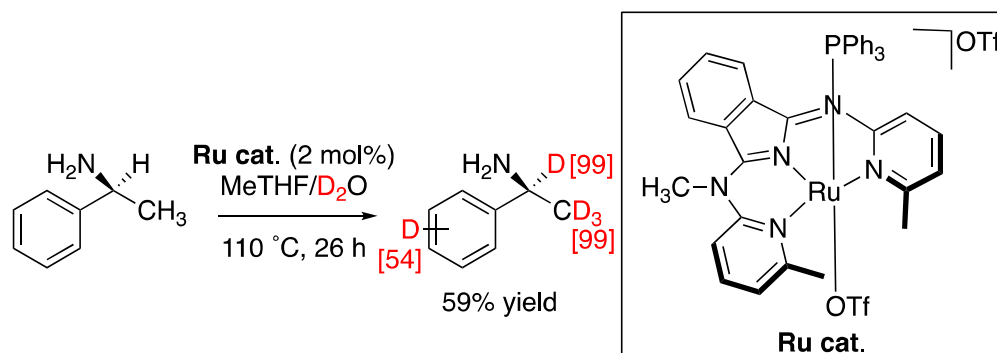
Deuterium ( $^2\text{H}$ ) is a rare and stable isotope of hydrogen, differing from protium by a single neutron and was first reported by Urey in 1932, who would later win the Nobel Prize in Chemistry in 1934 for his discovery of ‘heavy hydrogen’.<sup>1</sup> Interest in deuterated small molecules and the development of reactions to selectively install deuterium started gaining momentum around the 1990’s due to an increased demand for isotopically labelled compounds for spectroscopy and mass spectrometry (MS).<sup>2-5</sup> Since then, deuterated small molecules have gathered much attention as synthetic targets due to their wide variety of uses in both research and medicine. Isotopically labelled compounds are used to investigate organic and organometallic reaction mechanisms through kinetic isotope effect (KIE) studies.<sup>6-9</sup> These compounds are also used in biochemical studies to elucidate enzymatic and biosynthetic pathways.<sup>5, 10-17</sup> Molecules that are chiral by virtue of deuterium have been employed as stereochemical probes in metal-catalyzed transformations along with microbiological and enzymatic pathways.<sup>5, 10-24</sup>

Since the new millennium, deuterated bioisosteres have begun to broadly impact the study, design, and development of new medicines.<sup>3, 5, 25-29</sup> Deuterated small molecules have gained significant interest in medicine as candidates for new and enhanced therapeutics. The presence of deuterium in a bioactive organic molecule can alter the molecule’s pharmacokinetic properties including absorption, distribution, metabolism, and excretion (ADME).<sup>3, 25, 27, 29</sup> The potential of deuterated bioisosteres has already been demonstrated. As recently as 2017, the FDA approved the first deuterated small molecule

drug, deutetrabenazine, for the treatment of chorea associated with Huntington's disease and tardive dyskinesias.<sup>30</sup> Compared to the parent drug tetrabenazine, clinical trials for deutetrabenazine showed that the drug had a longer half-life in the body and required less frequent daily doses.<sup>31</sup>

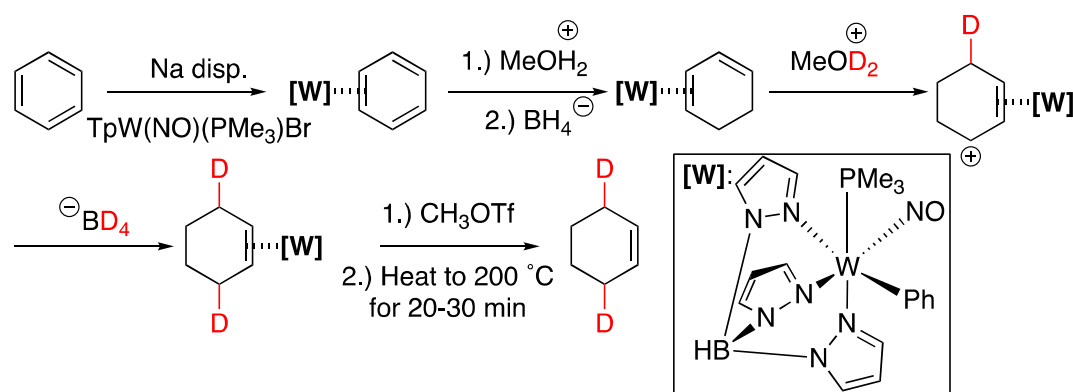
## 1.2 State-of-the-Art Methods for Installation of Deuterium into Small Organic Molecules

State-of-the-art techniques to selectively install deuterium into small molecules consist of metal-catalyzed hydrogen isotope exchange (HIE) and reductive deuteration processes. Despite substantial growth in the field of metal-catalyzed HIE, a significant challenge in this field is controlling the site-selectivity of these reactions (**Figure 1**). The drawbacks of this include excessive deuterium incorporation, which occurs when deuterium is incorporated into multiple different reactive C–H bonds within a substrate, or insufficient deuteration incorporation at the desired site.<sup>4, 32-37</sup> Heterogeneous catalysts used for HIE tend to be even less site-selective than homogenous catalysts because heterogeneous catalysts cannot exploit tunable ligands to control reactivity.<sup>4, 32, 38, 39</sup> To our knowledge, no enantioselective metal-catalyzed HIE methods have been reported.



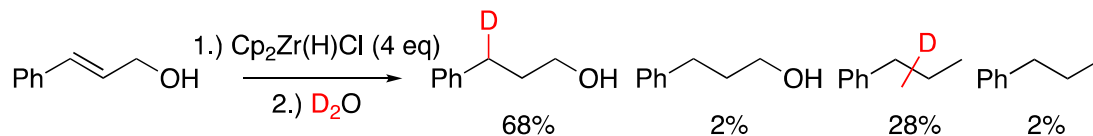
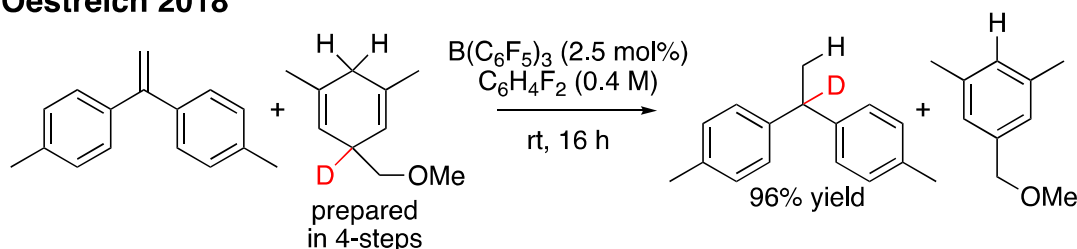
**Figure 1:** Metal-Catalyzed Stereoretentive Hydrogen Isotope Exchange<sup>36</sup>

State-of-the-art reductive deuteration methods have shown much promise for achieving high site-selectivity for deuterium installation. As recently as 2020, the Harman group showed that a benzene could undergo a four-step stereoselective transformation in the presence of stoichiometric tungsten complex with deuterated and proteated acid and hydride reagents (**Figure 2**).<sup>40</sup> Enantioselective deuteration using this method is not feasible because the tungsten complex remains strongly bound to the cyclohexene product and requires extreme temperatures (200 °C) in order to dissociate the complex.



**Figure 2:** Stereoselective Synthesis of Deuterated Cyclohexene Derivatives with a Tungsten Complex<sup>40</sup>

The Gronowitz group reported a moderately regioselective deuteration of an aryl alkene using stoichiometric Zr–H with a D<sub>2</sub>O workup (**Figure 3**).<sup>41</sup> This reaction results in multiple undesired side products, including the elimination of the hydroxyl group along with the dihydrogen product. Oestreich published a metal-free regioselective hydrodeuteration of aryl alkenes using monodeuterated 1,4-cyclohexadienes as a deuterium surrogate. This recent work serves as the first one-step selective regioselective transfer hydrodeuteration, but the method is limited to only to activated aryl alkenes.<sup>42, 43</sup>

**Gronowitz 1991****Oestreich 2018**

**Figure 3:** State-of-the-Art Regioselective Reductive Deuteration of an Aryl Alkenes<sup>41, 42</sup>

### 1.3 Chiral by Virtue of Deuterium Small Molecules

Although no metal-catalyzed methods for enantioselective deuteration using HIE or reductive deuteration have yet been presented, methods have been developed for the synthesis of enantioenriched chiral by virtue of deuterium small molecules. These methods exploit stereospecific, multi-step syntheses in order to convert enantioenriched starting materials to their respective deuterated products.<sup>24, 44-46</sup>  $\text{LiAlD}_4$  is used as a nucleophilic D-source in each of the discussed syntheses. The challenges presented in the synthetic routes and the limitations in available methods for the characterization highlight the level of difficulty required to obtain highly enantiopure chiral by virtue of deuterium molecules.

In 1949, Eliel showed that reduction of (–)- $\alpha$ -chloroethylbenzene with  $\text{LiAlD}_4$  yielded a product that showed an optical rotation value that was far in excess of possible observational error. That product was believed to be  $\alpha$ -deuteroethylbenzene (*dl*-ethylbenzene).<sup>44</sup> Inspired by this work, Mosher and coworkers developed a seven-step

stereospecific synthesis of (*S*)-*dl*-ethylbenzene product that starting from enantioenriched *R*-(-)-mandelic acid (100% ee) leveraging LiAlD<sub>4</sub> as the source of deuterium (**Figure 4**).<sup>45</sup> Although no absolute ee determination of (*S*)-*dl*-ethylbenzene was implemented, multiple optical rotation measurements were taken of both *dl*-ethylbenzene and the deuterated synthetic intermediates, demonstrating that molecules that are chiral by virtue of deuterium can rotate polarized light. The absolute (*S*) configuration of *dl*-ethylbenzene was rationalized by the authors due to the mechanistic pathway of the reactions employed.

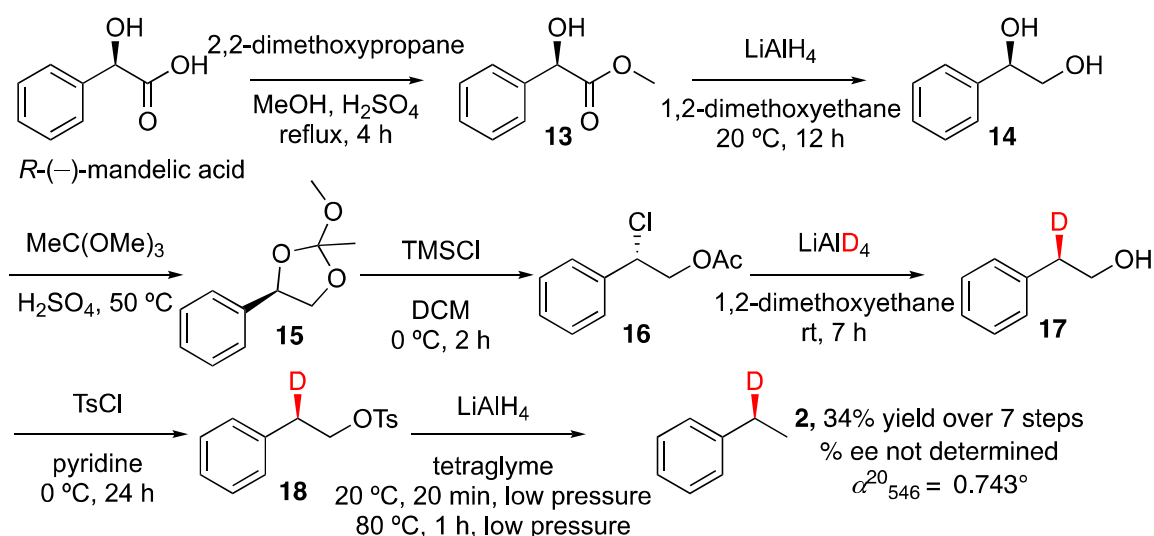


**Figure 4:** Mosher Synthesis of *dl*-Ethylbenzene<sup>45</sup>

Recently, the Christoffers group used a modified two-step procedure to synthesize (*S*)-*dl*-ethylbenzene from (*S*)-1-phenylethanol utilizing LiAlD<sub>4</sub> as the deuterium source (**Figure 5**).<sup>46</sup> Until this point, no absolute method had been used to determine the ee of *dl*-ethylbenzene and optical rotation measurements were used as the standard for determination of enantiopurity. Determination of optical rotation values has been

associated with errors, especially if the absolute values are relatively low.<sup>45</sup> Christoffers was unable to obtain a non-zero value for optical rotation for (*S*)-*d*1-ethylbenzene.

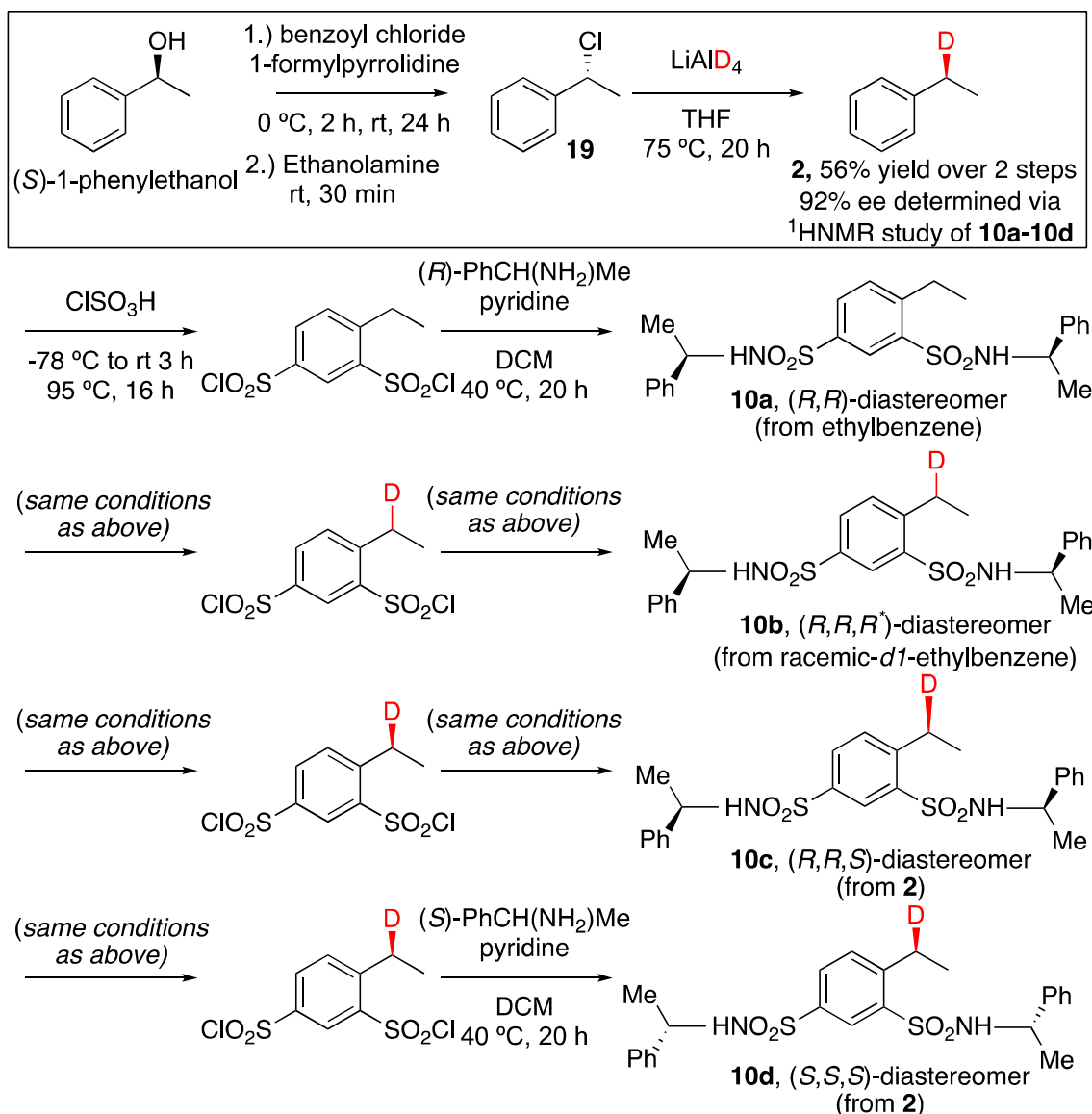


**Figure 5:** Christoffers Synthesis and derivatization of *dl*-Ethylbenzene<sup>46</sup>

Initially, a two-step derivatization of ethylbenzene (non-deuterated) by addition of a chiral *para*-substituted  $\alpha$ -phenylethyl sulfonamide motif was attempted to determine absolute ee through spectroscopic methods. The goal was to use a chiral auxiliary in close enough proximity to the benzylic carbon as to provide a chiral environment such that

separation of the methylene C–H  $^1\text{H}$  NMR peaks could be successfully distinguished. When observed via  $^1\text{H}$  NMR however, no resolute separation of the benzylic proton peaks was observed. This led to a challenging two-step derivatization to incorporate bis- $\alpha$ -phenylethyl sulfonamide diastereomers onto the aryl ring of ethylbenzene. Due to the deactivating effect of the first (*para*)sulfonyl-group, harsh conditions were required in order to obtain the second (*ortho*)sulfonyl-group (**Figure 5**).  $^1\text{H}$  NMR investigation of the bis-sulfonamide derivatized ethylbenzene **10a** showed two fully resolved quartet methylene proton peaks. The derivatization was then applied to racemic *dl*-ethylbenzene to give **10b**, and finally two separate derivatizations of (*S*)-*dl*-ethylbenzene were performed to give diastereomers **10c** and **10d** (**Figure 5**) which showed integrations of 1.00 ppm vs 0.04 ppm and 0.04 ppm vs 1.00 ppm respectively. From these integration values the authors determined that (*S*)-*dl*-ethylbenzene had a 92% ee.

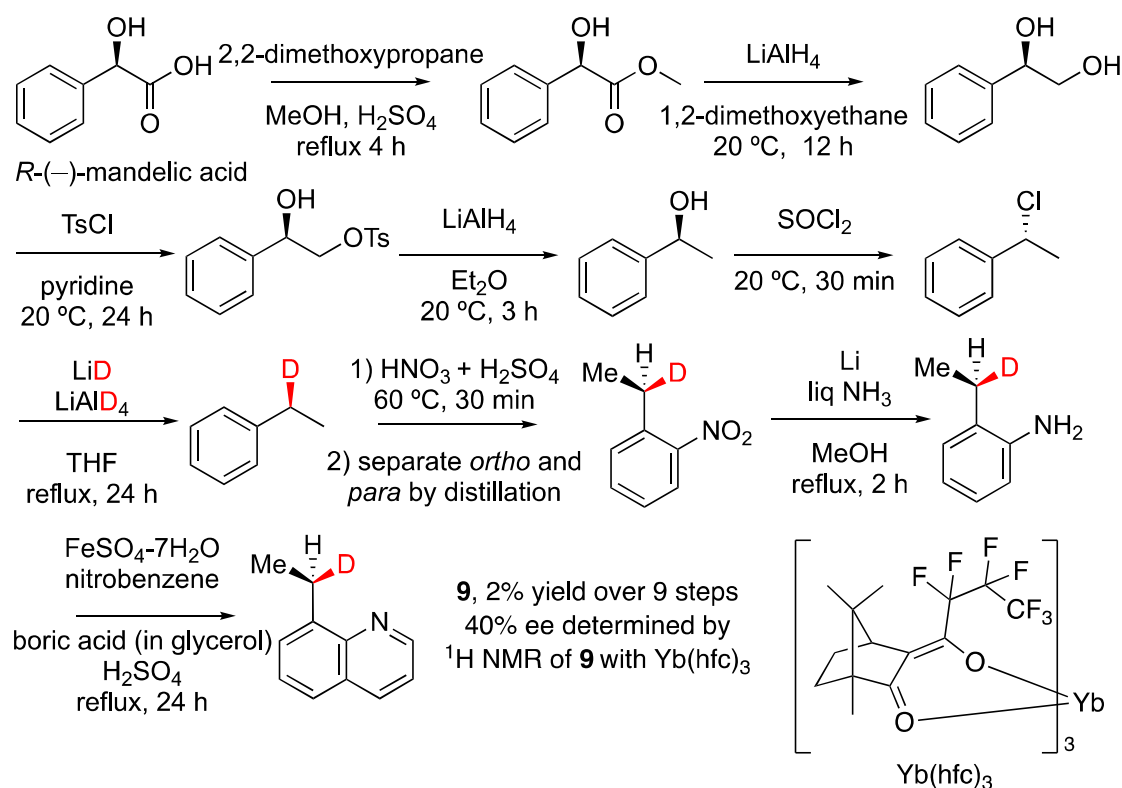


**Figure 6:** Flood's Synthesis of *dl*-(*R*)-(-)-8-( $\alpha$ -deuterioethyl)quinoline<sup>24</sup>

Flood and coworkers established a nine-step synthesis of (*R*)-(-)-8-( $\alpha$ -deuterioethyl)quinoline that invokes (*S*)-*dl*-ethylbenzene as a synthetic intermediate (**Figure 6**).<sup>24</sup> The synthetic route starts with *R*-(-)-mandelic acid and proceeds similarly to the Mosher and Christoffers syntheses of (*S*)-*dl*-ethylbenzene. Flood reported an 80% ee value for (*S*)-*dl*-ethylbenzene, determined by optical rotation. The optical rotation value determined by the Flood group ( $[\alpha]_{\text{D}}^{23} = -0.648^\circ$ ) is significantly lower than the value reported by Mosher ( $[\alpha]_{\text{D}}^{23} = -0.81^\circ$ ).<sup>45</sup> This discrepancy in optical rotation values supports the necessity for absolute methods for determining ee, especially with compounds that are chiral by virtue of deuterium. (*R*)-(-)-8-( $\alpha$ -Deuterioethyl)quinoline was determined to have a 40% ee, measured via  $^1\text{H NMR}$  study using a chiral shift reagent,  $\text{Yb}(\text{hfc})_3$  (**Figure 6**), that can coordinate with the Lewis basic nitrogen in the



quinoline ring to provide a chiral environment that results in methylene peak separation on  $^1\text{H}$  NMR and allows the benzylic peaks to be distinguished. It was hypothesized that the large drop in enantiopurity occurred during electrophilic nitration, but unfortunately the nitro moiety was not Lewis basic enough to bind with the chiral shift reagent.

#### **1.4 Research Objectives and Reaction Development**

Our research group focuses on new reaction discovery to enable the synthesis of novel pharmaceuticals and natural products. At the core of our research program is the development of selective transition metal-catalyzed reactions. My research in the group focuses on the synthesis and characterization of enantioenriched deuterated and fluorinated small molecules. Since deuterated small molecules have gained much attention for their wide variety of uses in chemical research and pharmaceuticals, there is a high demand for new methods to synthesize deuterated compounds. To the best of our knowledge, there exists no transition metal-catalyzed methods for the synthesis of chiral by virtue of deuterium small molecules.

The goal for our method development is to design a transition metal-catalyzed synthesis of chiral by virtue of deuterium small molecules in a highly regio- and enantioselective fashion (>90% ee) with little to no isotopic impurities and obtain these products in high yields. We also desired to find/develop a convenient, complementary method of characterization for our deuterated products that could allow us to quantify enantiopurity, isotopologue concentrations, and isotopomer distributions in our products, along with the capability of assigning absolute stereochemistry to the C–D stereogenic centers present in our products without the need for derivatizations that require lengthy or unnecessarily challenging synthetic overhead.

The challenge with constructing and optimizing a highly selective method for the synthesis of chiral by virtue of deuterium small molecules lies in the difficulty associated with characterization of these products. Optimization of new catalytic methods requires analytical techniques capable of high-throughput analysis, so that a battery of different reaction conditions and substrates can be probed until satisfactory reaction conditions can be determined.

Based on literature precedent of the Buchwald group in the field of hydroamination, our group proposed that an activated Cu–H complex could reduce an alkene to an alkane in combination with an electrophilic deuterium source.<sup>47, 48</sup> Until 2020, no examples of Cu–H's reducing alkynes or alkenes to alkanes exist to the best of our knowledge. Using an Ir-pincer complex, the Huang group was able to successfully reduce alkenes to alkanes, or deuterioalkanes, with EtOH or EtOD as the H or D source respectively.<sup>49</sup>

Recently, our group established efficient methods for Cu-catalyzed transfer hydrogenation and transfer deuteration of aryl alkynes (**Figure 7**).<sup>50</sup> These methods employ in-tandem either hydrosilane (Si–H) and isopropanol (<sup>i</sup>PrOH) or a deuteriosilane (Si–D) and <sup>i</sup>PrOD as sources of hydrogen or deuterium respectively. Although the reaction is not stereoselective, a bulky chiral bidentate phosphine ligand, (*R* or *S*)-DTBM-SEGPHOS, is used to enhance the reactivity of the Cu catalyst.

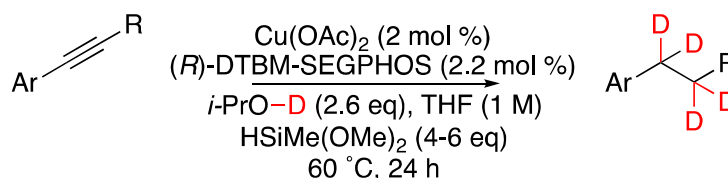


**Figure 7:** Cu-Catalyzed Transfer Deuteration of Aryl Alkynes<sup>50</sup>

Using these same principles, it was hypothesized that a regio- and enantio-selective transfer hydrodeuteration of aryl alkenes could proceed using a deuterated alcohol and a hydrosilane. In order to develop a regioselective hydrodeuteration, the Cu catalyst needs to discriminate between the H-source and D-source. The use of separate H-source (Si-H) and D-source allows for these chemicals to play separate roles in the catalytic cycle. It is well-documented that Si-H can promote *in situ* formation of Cu-H. (*R*)-DTBM-SEGPHOS is a bulky chiral ligand that could potentially provide sufficient enantioinduction to synthesize chiral by virtue of deuterium small molecules with high ee.

The proposed mechanism initiates with conversion of the Cu<sup>II</sup> precatalyst to active chiral ligand-bound Cu-H species after coordination of the phosphine ligand and transmetallation with Si-H (**Figure 8**). Hydrocupration of the active Cu-H species across the substrate aryl alkene  $\pi$ -bond occurs regioselectively to form the resonance stabilized benzylic Cu intermediate. Deuterodecupration should occur in the presence of a deuterated alcohol to release the chiral by virtue of deuterium product and the Cu catalyst will undergo another transmetallation with Si-H to regenerate the active Cu-H catalyst.

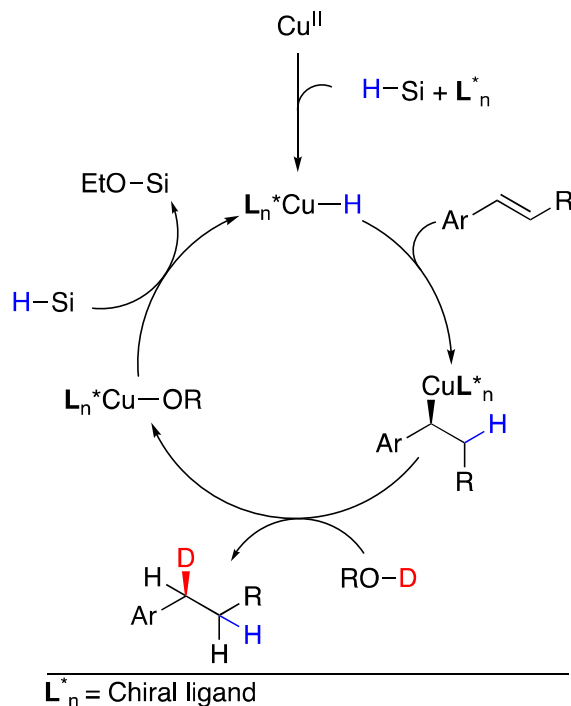


**Figure 8:** Proposed Mechanism for Enantioselective Cu-Catalyzed Hydrodeuteration of Aryl Alkenes

### 1.5 Chiral Analysis of Enantioenriched Chiral by Virtue of Deuterium Small Molecules using Molecular Rotational Resonance Spectroscopy

Molecular rotational resonance spectroscopy (MRR), also referred to as Fourier transform microwave spectroscopy, is a powerful spectroscopic tool with the capacity to differentiate between all types of isomers. MRR gives quantitative information about molecules in an analyte sample based on the molecule's mass distribution as quantified by the principal moments-of-inertia for overall rotation of that molecule in the gas phase.<sup>51-54</sup> At low pressure, molecules in the gas phase have quantized rotational angular momentum. This allows the analyte molecules to absorb and emit specific frequencies which will either increase or decrease the speed at which the analyte molecule rotates. These energy levels are sensitive to both the size and three-dimensional configuration of the analyte molecule. MRR can distinguish between regioisomers, stereoisomers,

isotopologues, and isotopomers to provide high-resolution spectroscopic data sufficient for the characterization of the analyte molecule.

MRR measurements are taken on either the broadband MRR instrument (left, **Figure 9**) or the IsoMRR instrument (right, **Figure 9**). The broadband instrument is a large hollow vacuum chamber that uses a micro- and milli- meter wave generator to transmit an excitation pulse throughout the chamber. The analyte molecules (sample to be analyzed) are introduced to the vacuum chamber via pulsed jet expansion, where analyte is dispersed from the sample well into the low-pressure cavity of the instrument by an inert carrier gas (usually neon gas). The gaseous analyte molecules are then excited and emit energy through free induction decay (FID) which can be detected and converted into a rotational spectrum.<sup>55</sup> The broadband MRR can detect a ‘broad’ range of the rotational spectrum in one round of data acquisition, taking a few hours per measurement, making this instrument useful for gathering the full rotational spectrum of new analyte molecules. The IsoMRR instrument has cavity enhanced instrument sensitivity for targeted measurements. IsoMRR provides high-throughput measurements compared to broadband with measurement times of about 10 minutes per sample and is an excellent tool for analyzing compounds that have established rotational spectra.



**Figure 9:** Broadband MRR Instrument and IsoMRR Instrument

Recently, MRR has been used for isotopomer and isotopologue analysis and was able to identify 15 different isotopic isomers in a sample at 100:1 dynamic range.<sup>40</sup> Since no two compounds (besides enantiomers) have the same MRR spectrum, crude samples can be directly injected for analysis without the need for purification. This is especially convenient in the case of resolving crude reaction mixture that contain isotopologues and isotopomers. Since enantiomers yield the same MRR spectrum, an enantioenriched ‘chiral tag’ molecule can be non-covalently bound to the analyte molecule as either a H-bond acceptor or H-bond donor. Once the tag molecule is bound to the analyte molecule, multiple diastereomers are formed, which will have unique rotational spectrums for each tag-analyte diastereomer complex formed. This technique allows for determination of ee and absolute configuration of analyte samples composed of a mixture of enantiomers.<sup>52, 54</sup> These characteristics of MRR make it a suitable and efficient method for analyzing molecules that are chiral by virtue of deuterium.

An accurate, high-throughput method for measuring ee, absolute configuration, and the presence of isotopic impurities of our deuterated products is necessary for further optimization of the transfer hydrodeuteration protocol and expansion of the substrate scope. MRR showed immense potential as an analytical technique that can meet these demands. For this reason, our group established a collaboration with experts in the field of rotational spectroscopy, the Pate group at the University of Virginia and BrightSpec Inc.

Initial studies commenced with a silyl protected cinnamyl alcohol derivative as the aryl alkene (**Figure 10**). This substrate was originally selected since the hydroxyl group can serve as a Lewis basic coordination site for chiral shift reagents or as a

functional handle for installation of a chiral auxiliary for  $^1\text{H}$  NMR studies. A free alcohol will compete with the deuterated alcohol in the deuterodecupration step of the proposed reaction mechanism, therefore, the alcohol was converted to its respective silyl ether prior to being subjected to catalysis. A  $\text{Cu}(\text{OAc})_2$  precatalyst was selected with (*R*)-DTBM-SEGPHOS as a chiral ligand and dimethoxymethylsilane (DMMS) as the Si–H source to form the active chiral Cu–H catalyst. EtO–D was used as the source of deuterium and the reaction was run at 40 °C in tetrahydrofuran (THF). Deuterated cinnamyl alcohol **1b** was isolated in 77% yield (over two-steps, **Figure 10**).  $^1\text{H}$  and  $^{13}\text{C}$  NMR were used to evaluate the extent of deuterium incorporation into the benzylic position of the product and to look for isotopic impurities. No evidence of deuterium incorporation into the homobenzylic position was observed by NMR analysis.

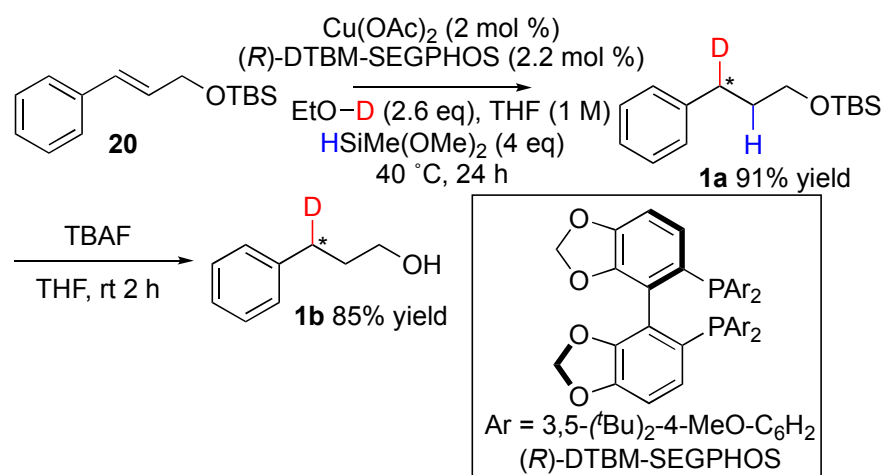


**Figure 10:** Initial Study of Catalytic Regio- and Enantio- Selective Aryl Alkene Transfer Deuteration

The product from our initial study, *d*l-3-phenylpropanol, served as the first substrate subjected to MRR analysis. Since enantiomers have the same rotational spectra,

a chiral tag must be bound to the deuterated analyte molecule to form diastereomers, each with a unique and distinguishable rotational spectrum, which enables measurements of ee and the determination of absolute configuration. Propylene oxide was chosen as an optimal chiral tag due to its ability form a strong non-covalent H-bond with the alcohol motif on *dl*-3-phenylpropanol. Once a suitable tag was identified, quantum chemical analysis using dispersion corrected density functional theory (B2PLYPD3 def2TZVP) was utilized, which predicts the dominant spectra based on the lowest energy analyte-tag complexes (**Figure 11**).<sup>56</sup> Once valid theoretical structures were established, initial measurements were taken with a racemic propylene oxide tag, which bound to either enantiomer of analyte and form one of four possible diastereomer complexes, two homochiral complexes where the assigned absolute stereochemistry of the tag and analyte are the same (*R,R* or *S,S*), and two heterochiral complexes where the assigned stereochemistry of the tag and analyte are opposite (*R,S* or *S,R*) (eq. (1), **Figure 12**). Homochiral and heterochiral transition peaks were observed to ensure that equal densities of diastereomer complexes were formed in the pulsed jet expansion and that the transition signal frequencies predicted by quantum chemistry matched the experimentally observed transition frequencies.



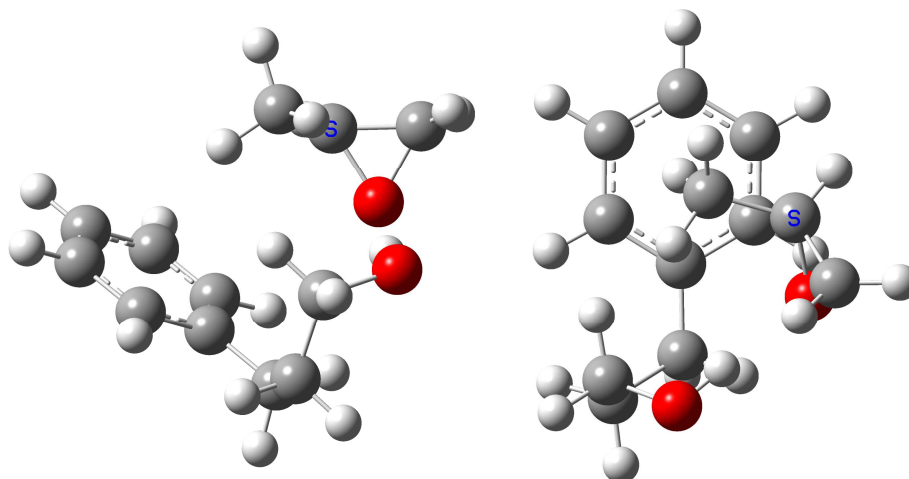


**Figure 11:** Sample 3-D Models of Chiral Tag-Analyte Diastereomer Complexes

Upon verification of homochiral and heterochiral transitions using racemic propylene oxide, highly enantiopure (*S*)-propylene oxide (99.6% ee) was used for chiral analysis, which formed one homochiral and one heterochiral complex (eq. (2), **Figure 12**). If the *dl*-3-phenylpropanol sample is a high enantiopurity, then one of the diastereomer complexes will display a significantly higher transition intensity relative to the less abundant diastereomer. In **Fig. 13**, the top two spectra show the transient signals for the homochiral (labelled red) and heterochiral complexes (labelled blue) when racemic propylene oxide was used while the bottom two spectra show the homochiral and heterochiral transient signals when (*S*)-propylene oxide was used. Background transition lines in **Fig. 13** have been colored grey for aesthetic purposes. These transition lines represent various complexes such as non-dominant analyte-tag conformers, analyte-water or tag-water complexes, substrate or tag dimerization, or possible impurities present in the analyte sample (**Figure 13**).

Once the rotational spectrum was generated using enantiopure tag, the ratio of homochiral to heterochiral transition signal intensities was then averaged across multiple

signals to determine the ee of *d1*-3-phenylpropanol. Since the geometries of the complexes associated with each signal were known via quantum chemistry, the absolute stereochemistry was assigned accordingly based on the stereochemistry of the dominant diastereomer complex.

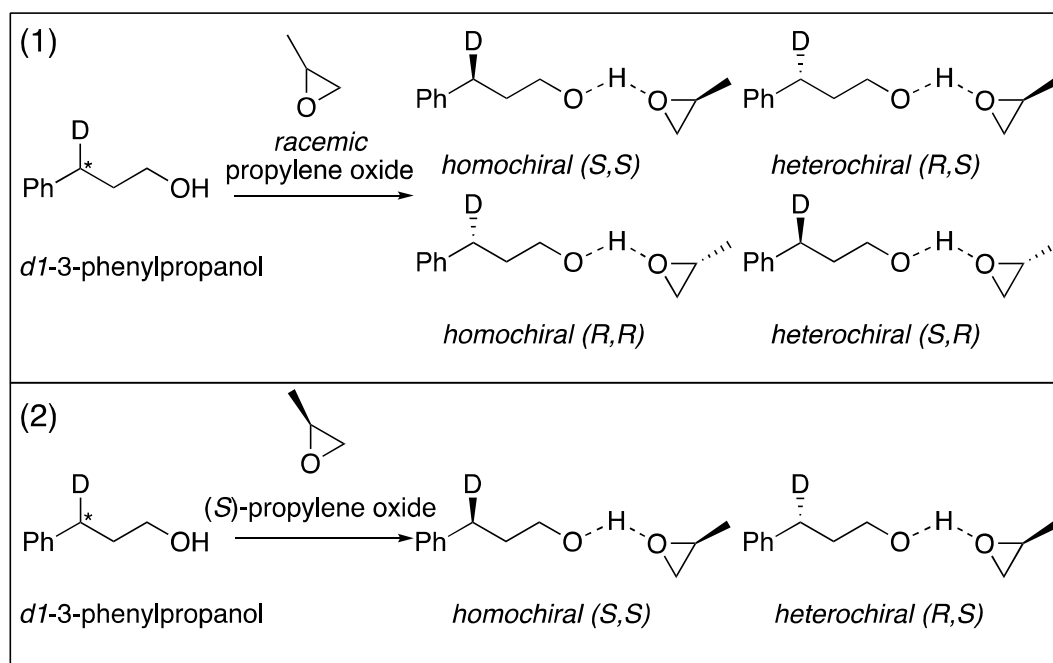


**Figure 12:** Formation of Homochiral and Heterochiral Diastereomer Substrate-Tag Complexes for MRR analysis

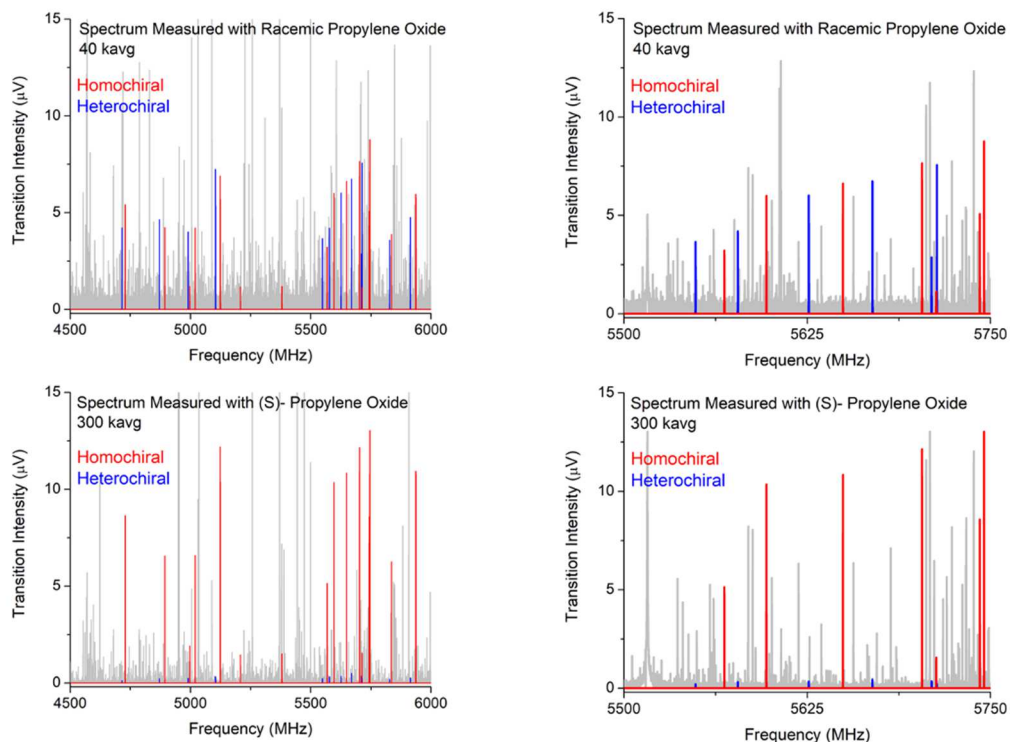


**Figure 13:** MRR Spectra of *dl*-3-Phenylpropanol with Racemic Propylene Oxide and (*S*)-Propylene Oxide

MRR measured *dl*-3-phenylpropanol to have a 98% ee by direct comparison of multiple transition signal intensities between corresponding heterochiral (top left and bottom left spectra, **Figure 14**) and homochiral (top right and bottom right spectra, **Figure 14**) complexes formed with (*S*)-propylene oxide. Quantum analysis of the absolute stereochemistry of the prevailing enantiomer indicated that the (*S*) enantiomer was formed in excess. MRR analysis by the Pate group determined that the product contained only 0.1% isotopic impurity consisting of both the dihydrogen species (where H inserts in to both the benzylic and homobenzylic position) and regioisomer impurity (D incorporated at the homobenzylic position).

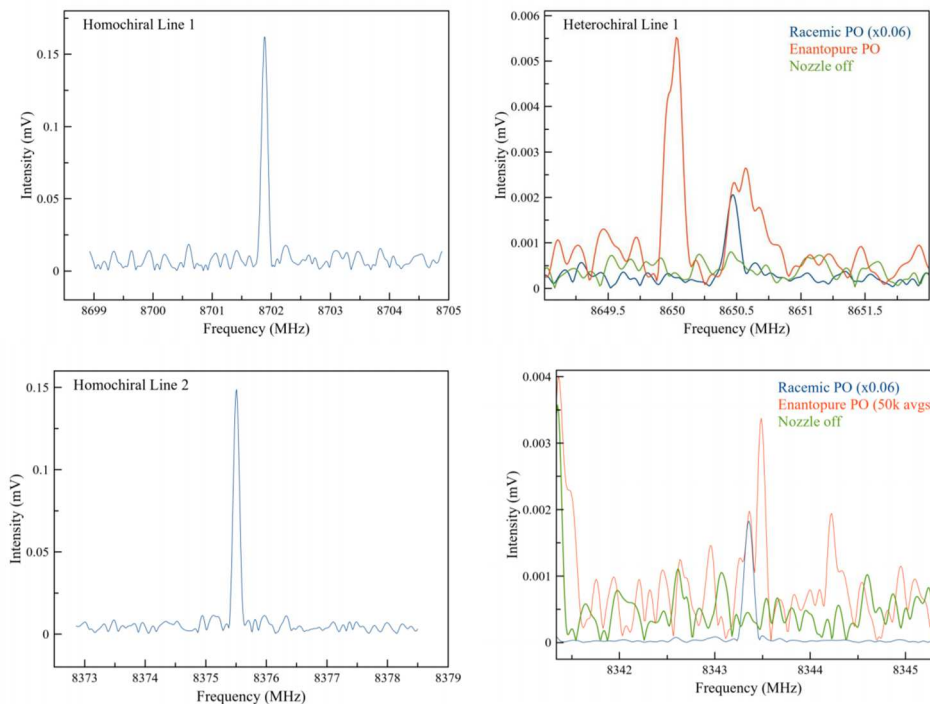


**Figure 14:** Zoomed in Comparison of Homochiral and Heterochiral Transition Signals with (*S*)-Propylene Oxide

## 1.6 Synthesis and Chiral MRR Analysis of *dl*-Ethylbenzene

To demonstrate the validity of using MRR for chiral analysis, we wanted to analyze and compare the ee's of *dl*-ethylbenzene prepared using Mosher's and Christoffers' method.<sup>45, 46</sup> We also wanted to prepare *dl*-ethylbenzene from commercially available styrene using our catalytic transfer hydrodeuteration to submit for MRR analysis. Both Mosher and Christoffers synthesis of *dl*-ethylbenzene are multiple steps and employ LiAlD<sub>4</sub> as the source of deuterium. LiAlD<sub>4</sub> cost upwards of \$335 per gram (aablocks), while the deuterated ethanol used in our catalytic cycle is only \$46 per 25 mL (Millipore Sigma). Transfer hydrodeuteration could offer a more cost-efficient method to synthesize chiral by virtue of deuterium small molecules in one-step while simultaneously reducing synthetic overhead.

Following the exact synthetic route taken by both Mosher and Christoffers, *dl*-ethylbenzene was successfully synthesized with a 1.5% yield over seven-steps following Mosher's method and 35% yield over two-steps following Christoffers method (**Figure 4 and 5**).<sup>45, 46</sup> Cheap, commercially available styrene (\$33.20 per liter from Millipore Sigma) underwent full conversion to the deuterated alkane when subjected to the same catalytic conditions as *dl*-3-phenylpropanol, except poly(methylhydrosiloxane) was used as a milder and less toxic source of Si-H (**Figure 10**). The reaction was run at gram-scale and, after purification, *dl*-ethylbenzene was obtained in 53% yield in one-step. It should be noted that the yield for this substrate was significantly lower than the other aryl alkene substrates due to its high volatility.

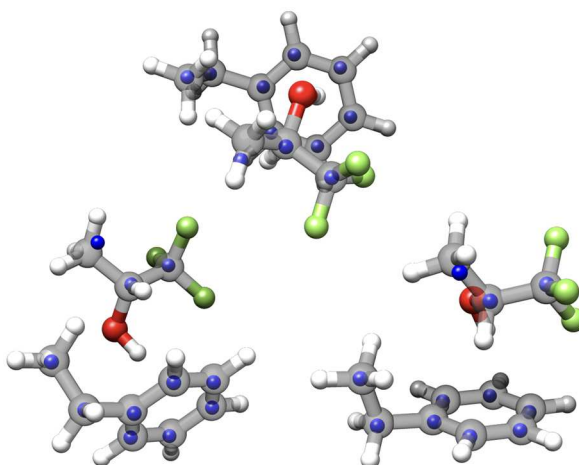


**Figure 15:** Sample 3-D Models of Chiral Tag-Analyte Diastereomer Complexes

Three samples of *dl*-ethylbenzene synthesized using the various methods were then submitted for MRR isotopic analysis. Trifluoroisopropanol (TFIP), was selected as the tag because the hydroxyl group of TFIP was able to form a H-bond with the benzene ring of ethylbenzene. After quantum analysis using DFT,<sup>56</sup> the lowest energy complexes were determined and racemic TFIP was used to determine the heterochiral and

homochiral transient species (**Figure 15 and 16**). Addition of enantioenriched (*S*)-TFIP (99.3% ee) resulted in almost

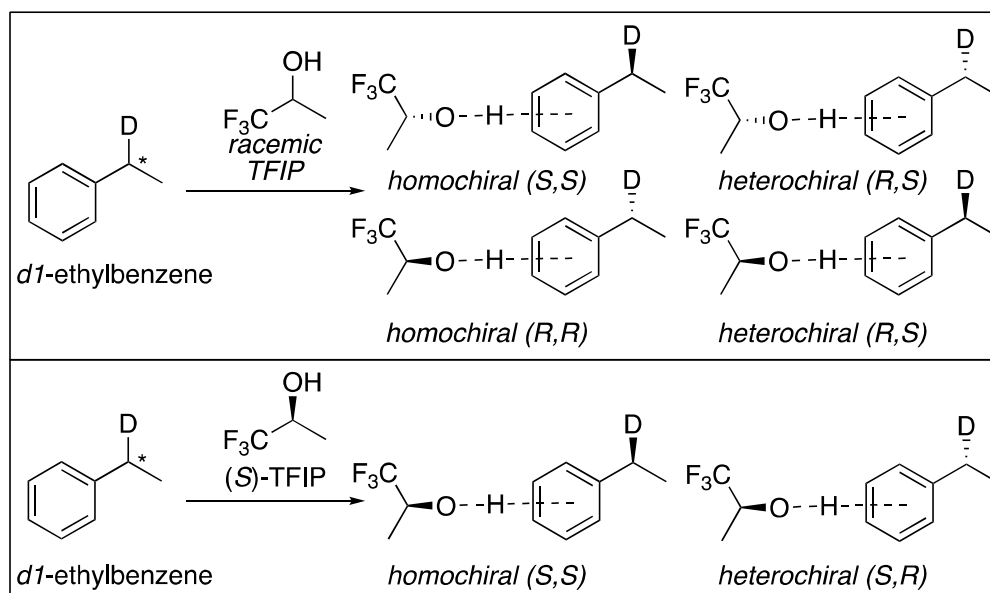


**Figure 16:** Formation of Homochiral and Heterochiral Diastereomer Substrate-Tag Complexes for MRR Analysis

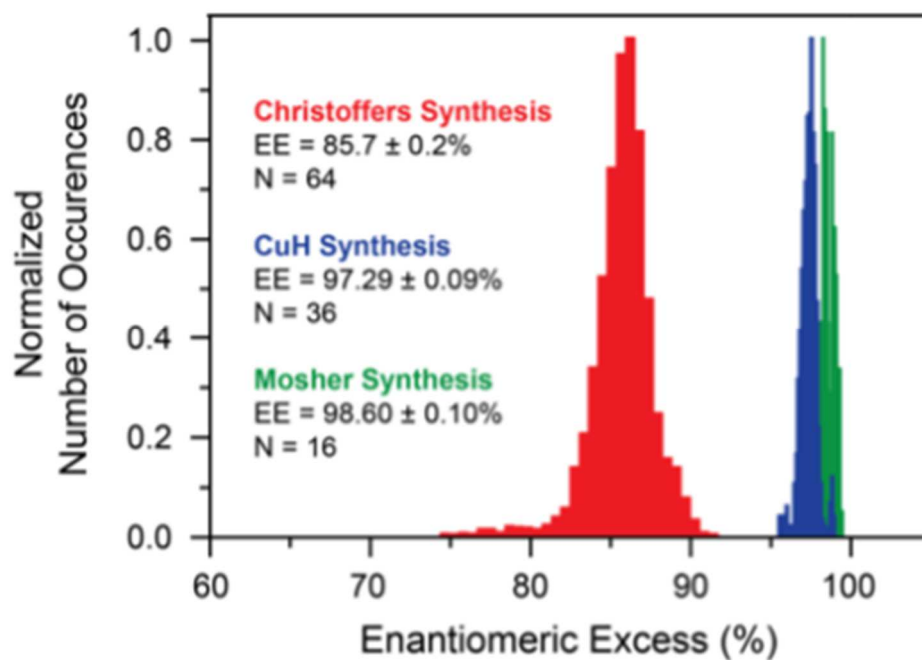


**Figure 17:** Summary of MRR Chiral Analysis of *d1*-Ethylbenzene Samples

exclusively the homochiral (*S,S*) transient species for all three *dl*-ethylbenzene samples. The absolute stereochemistry for all three ethylbenzene samples was determined to be (*S*), with the ee for the Mosher sample, Christoffers sample, and transfer hydrodeuteration sample were 98.60% ee, 85.7% ee, and 97.29% ee respectively (**Figure 17 and 18**). Our transfer hydrodeuteration provides highly enantiopure (*S*)-*dl*-ethylbenzene in just one-step on gram scale.

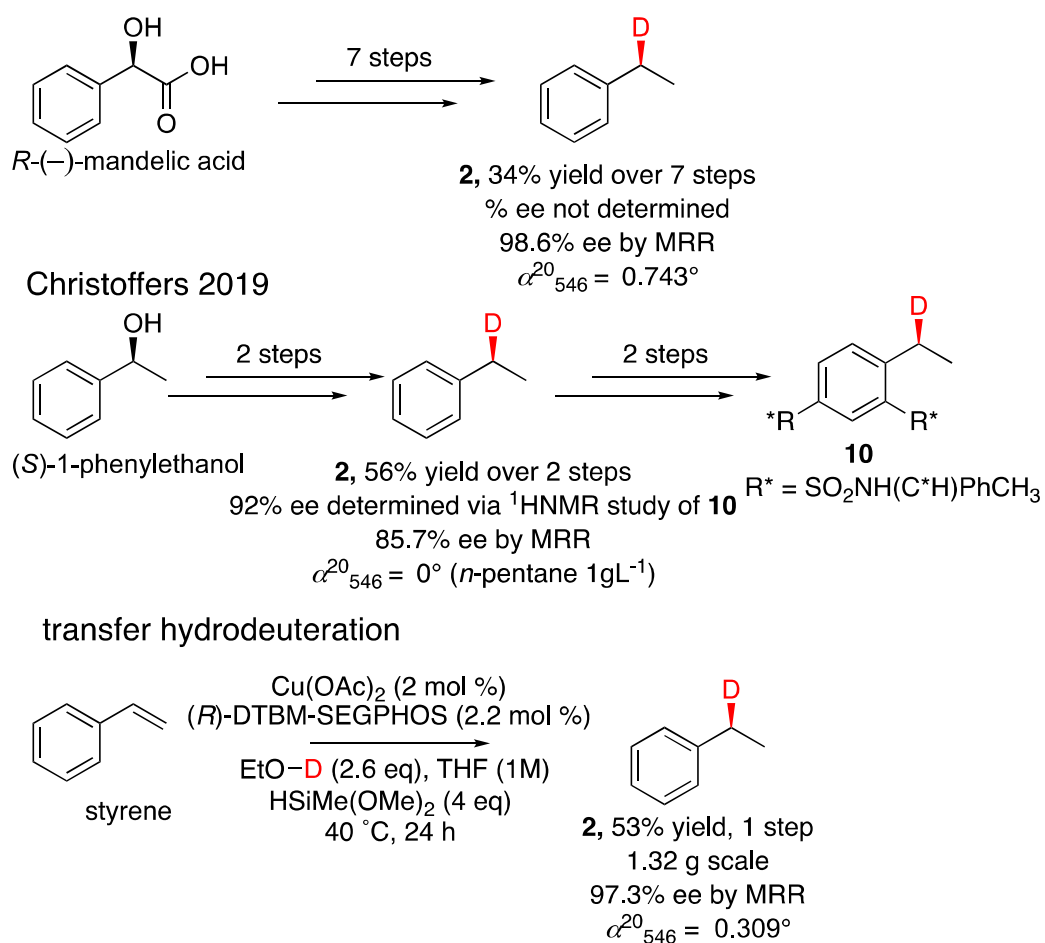


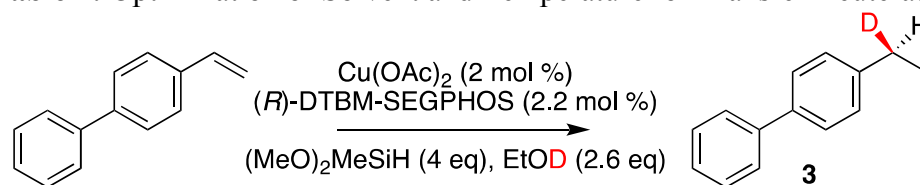
**Figure 18:** Comparison of Synthetic Routes and EE's of (*S*)-*dl*-Ethylbenzene using MRR Analysis<sup>45, 46</sup>

## 1.7 Reaction Optimization and Substrate Scope

The success of our enantioselective catalytic transfer hydrodeuteration lead us to further expand the substrate scope. Full conversion of 4-Vinylbiphenyl to *dl*-4-ethylbiphenyl was observed under transfer hydrodeuteration conditions. Chiral analysis of *dl*-4-ethylbiphenyl by MRR using (*S*)-TFIP as a chiral tag showed 77% ee and was assigned an absolute stereochemistry of (*S*). 4-Vinylbiphenyl was chosen as the substrate for optimization as it did not have >90% ee (entry 1, 85% yield, **Table 1**).

Different solvents, solvent combinations, solvent concentrations and reaction temperatures were explored to investigate their effect on ee. When reacted at room temperature or in a cold room (°5 C), a substantial increase in ee was measured for *dl*-4-ethylbiphenyl (92% ee entry 2, 96% ee entry 3, **Table 1**). Other solvents, including 1,4-dioxanes, solvent mixtures using different ratios of 1,4-dioxane and THF, and methyl *t*-butyl ether (MTBE) all showed exceptional ee's of >90% (entries 5-9). Running the reaction more dilute showed an inverse effect on ee (entry 4). MRR spectroscopy enables high-confidence and high-throughput methods for analysis of chiral by virtue of deuterium small molecules, with each ee measurement taking on-average 10 minutes.



**Table 1:** Optimization of Solvent and Temperature for Transfer Deuteration

Entry	Solvent <sup>a</sup>	Concentration <sup>b</sup>	Temp.	% Yield <b>X</b>	% ee <b>X</b>
1	THF	1 M	40 °C	85%	77%
2	THF	1 M	rt	80%	92%
3	THF	1 M	5 °C	98%	96%
4	THF	0.5 M	40 °C	76%	67%
5	1,4-dioxanes	1 M	40 °C	90%	85%
6	4:1 (d:t)	1 M	40 °C	95%	85%
7	1:1 (d:t)	1 M	40 °C	99%	91%
8	1:4 (d:t)	1 M	40 °C	96%	92%
9	MTBE	1 M	40 °C	94%	88%

<sup>a</sup>d:t (1,4-dioxane:THF) <sup>b</sup>Based on 0.5 mmol substrate

With optimized reaction conditions in hand, reactivity of various aromatic and heteroaromatic alkenes were probed (**Figure 19**). Along with aforementioned substrates, naphthalene, methoxynaphthalene, and benzofuran substituted aryl alkenes were all synthesized in excellent yields with high ee's (substrates **1-6**, **Figure 19**). Nitrogen containing heterocycles were obtained in moderate to good yields, however a significant loss of ee was observed for these substrates (substrates **7-9**). It was hypothesized that the lone pairs of electrons on N could competitively bind to the metal catalyst and cause dissociation of the chiral ligand. If this is the case, then transfer hydrodeuteration would occur via a nonchiral catalyst, resulting in lower ee or even racemic product mixtures.

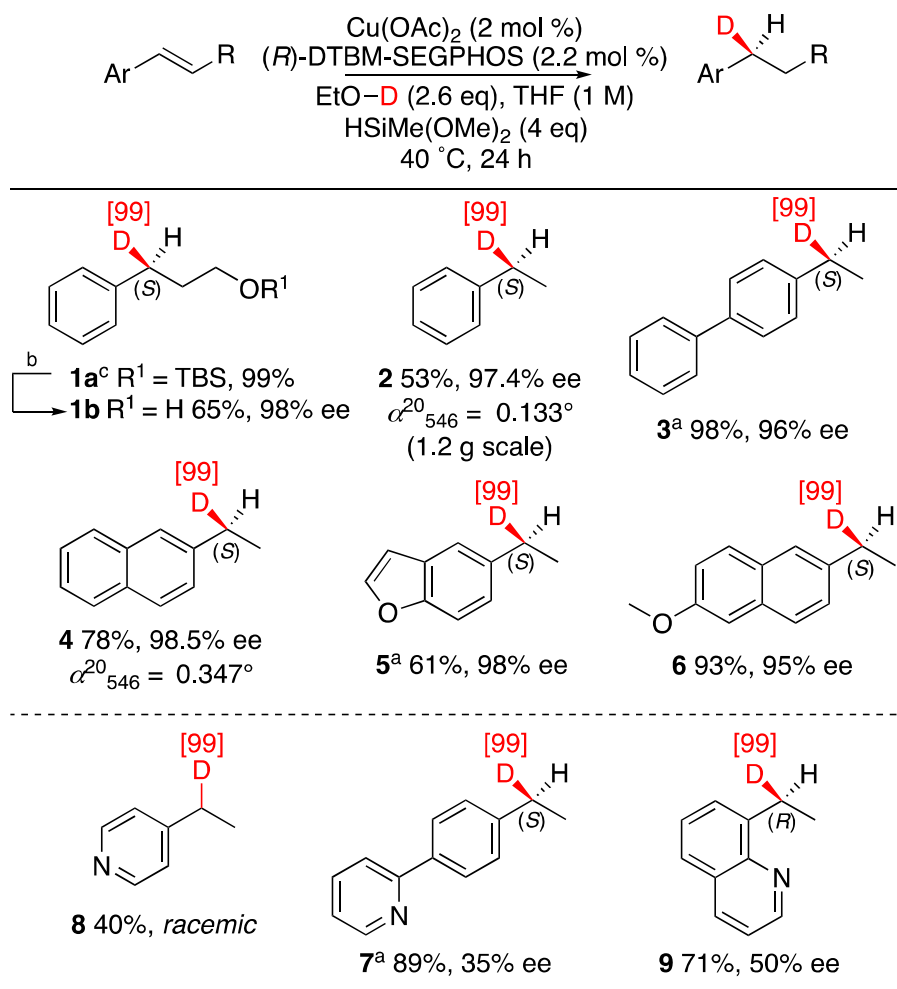


**Figure 19:** Transfer Hydrodeuteration Substrate Scope

### 1.8 Future Work

Future work for this product will focus on expansion of the alkene substrate scope (**Figure 20**). We have devised several experiments to study and enhance reactivity of N-containing heterocycles in our reaction. To investigate our hypothesis of competitive N-binding to our catalyst, DTBM-SEGPHOS will be replaced with catalytic amounts of 4-ethyl pyridine to see if a N-containing heterocycle can catalyze the transfer deuteration with our Cu precatalyst. Since the N-lone pair may be coordinating to our catalyst,

quaternization of the N using  $\text{BF}_3 \cdot \text{OEt}_2$  could minimize this interaction, allowing the intended chiral catalyst to perform the reaction (**Figure 21**).

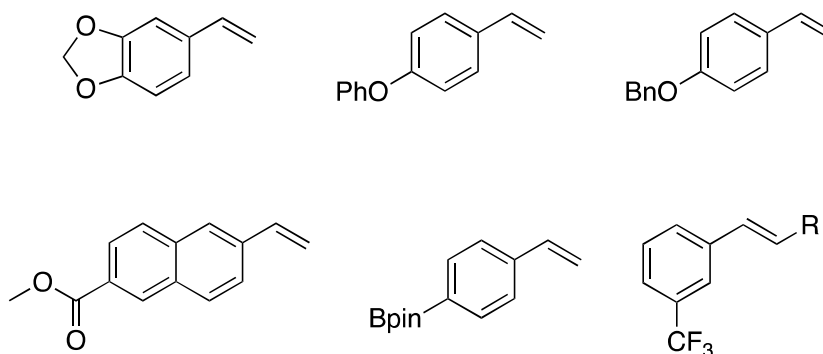


**Figure 20:** Future Substrate Scope for Transfer Hydrodeuteration Project

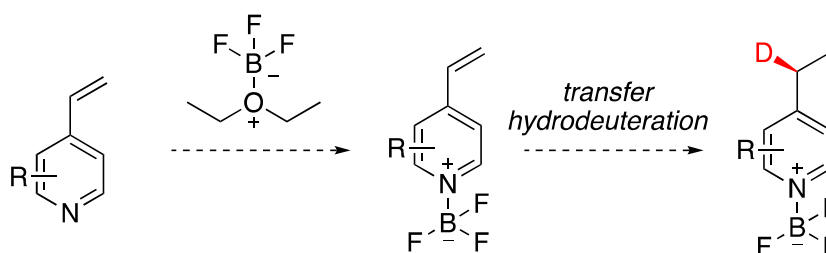


**Figure 21:** N-Quaternization Strategy for Improved Enantioselectivity of N-Containing Heteroaryl Alkenes

We believe that MRR has the potential to exist at the forefront of spectroscopic methods for ee determination, isotopologue characterization, and isotopic impurity measurements for small organic molecules. To demonstrate this, we will recreate Flood's synthesis of (*R*)-(-)-8-( $\alpha$ -deuterioethyl)quinoline to determine which step (or steps) in the synthetic route the significant loss of enantiopurity occurs (**Figure 6**).<sup>24</sup> Flood measured the ratio of enantiomers for both (*R*)-(-)-8-( $\alpha$ -deuterioethyl)quinoline and its synthetic precursor (*R*)-*ortho*-( $\alpha$ -deuterioethyl)-aniline by  $^1\text{H}$  NMR using peak deconvolution in the presence of a chiral shift reagent. The other deuterated synthetic intermediates lacked

the presence of a strong enough Lewis base to generate pseudo-contact shifts with the chiral shift reagent, leaving Flood to hypothesize that loss of enantiopurity occurred in the electrophilic nitration step of the synthesis. We hypothesize that using the chiral tag methodology, MRR will be able to accurately quantify the enantiopurity of each of these chiral by virtue of deuterium synthetic intermediates. It should also be noted that the authors reported an 80% ee for (*S*)-*dl*-ethylbenzene, which is not consistent with the value previously reported by Mosher.<sup>45</sup> This suggests that there may be a degree of error associated with ee measurements taken exclusively from optical rotation values.

## Chapter 2: Cu-Catalyzed Enantioselective Hydrofluorination of Alkenyl Arenes

### 2.1 Introduction

Organofluorines have dominated the pharmaceutical and agrochemical marketplace since the arrival of fludrocortisone (Fluorinef acetate) in 1954. Blockbuster drugs such as atorvastatin (Lipitor), fluoxetine (Prozac), and paliperidone palmitate (Invega Sustenna) all contain at least one fluorine atom (**Figure 22**).<sup>57-58</sup> Approximate 20% of all commercially available pharmaceuticals and an even higher 30% of agrochemicals contain at least one fluorine.<sup>57, 58, 60, 61</sup> In 2018 and 2019, 40% of the new FDA approved small molecule drugs contain fluorine.<sup>60</sup> While more than half of the FDA approved fluorine-containing drugs in 2019 contain a stereocenter, less than 1% of these drugs contain a C-F stereocenter.<sup>58, 59</sup> All of the chiral drugs containing a stereogenic C(sp<sup>3</sup>)-F bond are cyclic fluorinated compounds with limited structural diversity.<sup>58</sup>

Deliberate incorporation of fluorine into specific positions within a bioactive molecule is a fundamental principle in the synthesis of unique bioisosteres.<sup>25, 29</sup>

Organofluorine bioisosteres are in such high demand because fluorine substitution can alter  $pK_a$ , enhance lipophilicity and influence metabolism, potency, conformation and membrane permeability of a bioactive molecule.<sup>57-60</sup> Unfortunately, fluorinated organic molecules occur scarcely in nature and are the least abundant organohalides.<sup>13</sup> Only 21 biosynthesized, fluorine-containing molecules have been isolated and only a single enzyme (5'-fluoro-5'-deoxyadenosine synthase) capable of fluorination is known.<sup>62, 63</sup> Ionic fluorine is a potent nucleophile in aprotic environments, however in aqueous media the fluorine ion is tightly hydrated and effectively inert. Additionally, fluorine's high redox potential excludes haloperoxidase-type mechanisms seen in the metabolic incorporation of bromine and chlorine.<sup>64-66</sup> Lack of bioavailable fluorinated small molecules places the burden on synthetic chemists to develop selective fluorination methods to meet the growing demands for fluorinated bioisosteres.

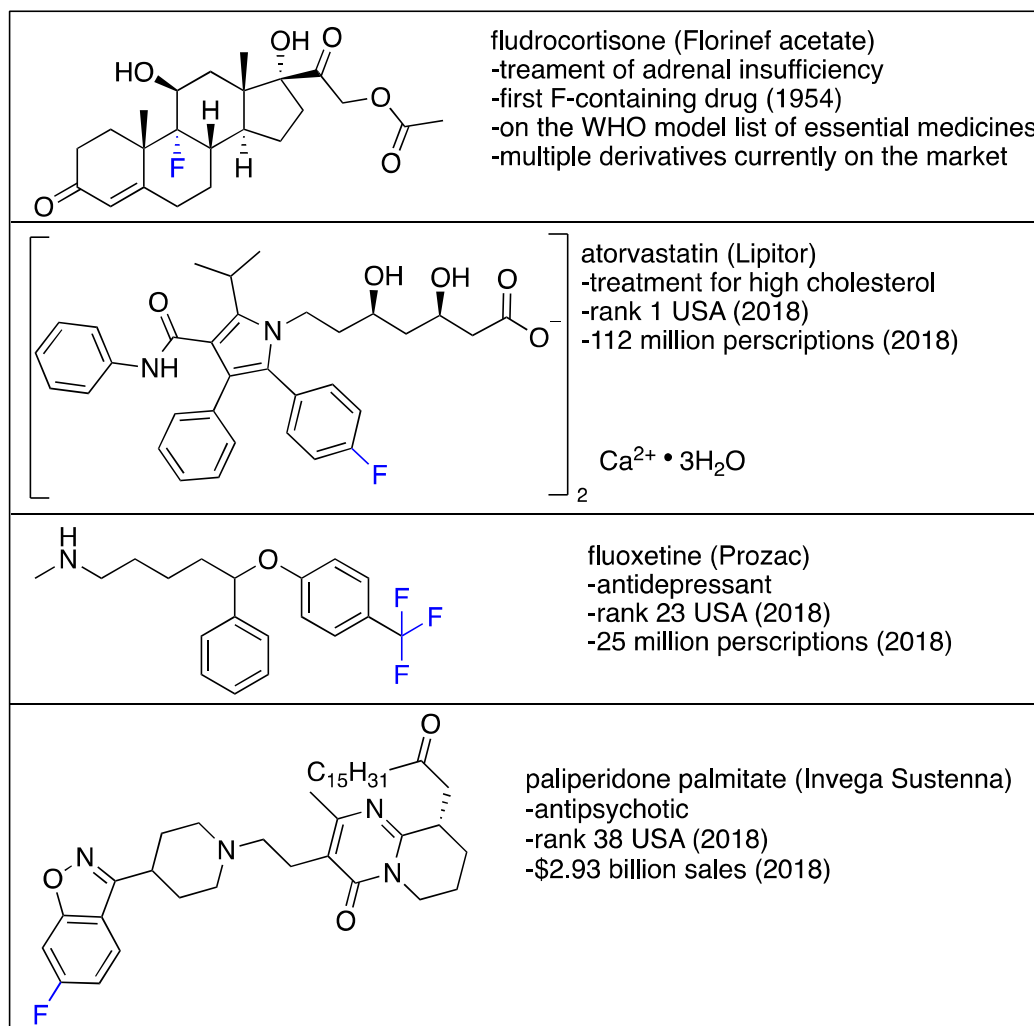


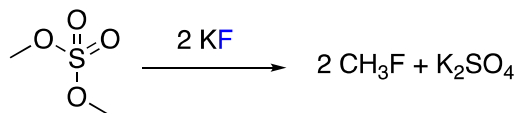
**Figure 22:** Blockbuster Organofluorine Commercial Drugs

## 2.2 History of Fluorination and State-of-the-Art Methods for Metal-Catalyzed Hydrofluorinations

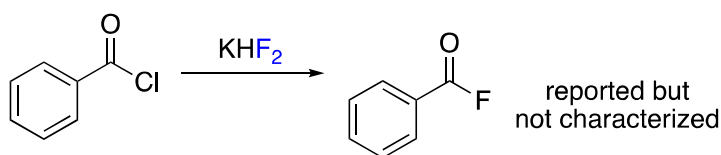
Inorganic fluorides have been recognized since the 16<sup>th</sup> century and hydrofluoric acid was reported in the 17<sup>th</sup> century, however, due to the absence of fluorine in biology and the harsh nature of early fluorinating reagents, organofluorine chemistry was not born until the mid-19<sup>th</sup> century.<sup>67,68</sup> Moissan is credited with the discovery of fluorine for first isolating elemental fluorine in 1886 as dry hydrofluoric acid and potassium difluoride (HF and KHF<sub>2</sub>).<sup>68, 69</sup> In 1835 (Dumas *et al*) and 1862 (Borodin) claim to have synthesized

the first organofluorine by nucleophilic substitution of an acid chloride using an inorganic source of fluorine (KF and KHF<sub>2</sub> respectively, **Figure 23**).<sup>67, 68</sup>

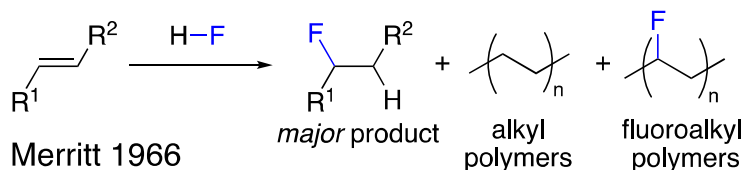
Dumas 1835



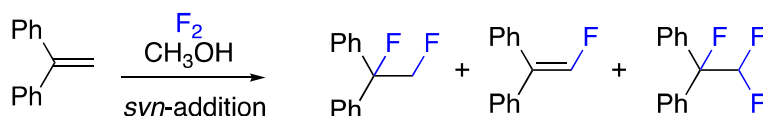
Borodin 1862



Grosse and Linn 1938



Merritt 1966

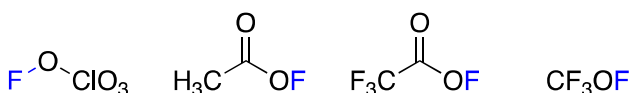


**Figure 23:** Pioneering Work in Alkene Fluorination<sup>66-68, 70</sup>

Early fluorination chemistry utilized inorganic fluorinating reagents such as metal fluorides, HF, and F<sub>2</sub>.<sup>66, 70</sup> Grosse and Linn used HF to accomplish the first recorded hydrofluorination of an alkene to corresponding fluoroalkane (**Figure 23**).<sup>66</sup> Later, Merritt was able to synthesize difluoroalkanes from respective olefins using elemental fluorine gas in methanol.<sup>70</sup> HF mediated hydrofluorination of an alkene and alkene difluorination suffer from two distinct setbacks: (1) highly reactive fluorine reagents results in low selectivity and functional group tolerance. Fluorinations involving HF and F<sub>2</sub> give multiple undesired side products in most cases. (**Figure 23**), (2) Both HF and F<sub>2</sub>

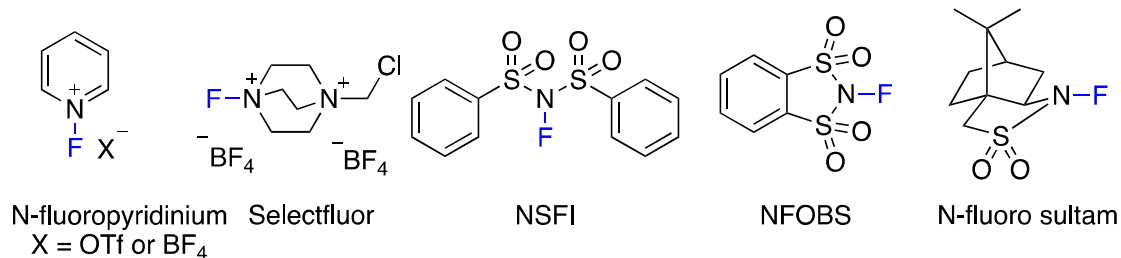
are notoriously dangerous chemicals to work with. HF is highly corrosive and potentially fatal if ingested or inhaled, handling of this chemical requires specialized equipment since it reacts with both metal and glass. F<sub>2</sub> was especially infamous at the time because gaseous fluorine is highly toxic, flammable, and reacted violently with water to form HF.

inorganic reagents: AgF<sub>2</sub>, CoF<sub>3</sub>, CsSO<sub>4</sub>F, HgF<sub>2</sub>, RbSO<sub>4</sub>F, PbF<sub>2</sub>(OAc)<sub>2</sub>

hypofluorites: 

ammonium fluorides: Et<sub>3</sub>N•3HF, Pyridine•HF

N-fluoro reagents:



nucleophilic: Et<sub>2</sub>NSF<sub>3</sub> (DAST), (Me<sub>2</sub>N)<sub>3</sub>S(Me)<sub>3</sub>SiF<sub>2</sub>

other F-reagents: PhIF<sub>2</sub>, BF<sub>3</sub>, XeF<sub>2</sub>, F<sub>2</sub>, HF

**Figure 24:** Fluorinating Reagents<sup>71</sup>

Many organic chemists outright avoided these chemicals, inspiring the development of safer and less reactive fluorinating reagents. The evolution of fluorine chemistry and fluorinating reagents has been synonymous. Early efforts in organofluorine chemistry targeted production of safer and more bench stable fluorinating reagents. This caused a shift from inorganic fluorine sources to hypofluorites, which contain an electrophilic O–F bond (**Figure 24**).<sup>71</sup> Hypofluorites and ammonium fluorides ushered in new synthetic protocols, allowing for safer procedures to explore and expand fluorination chemistry,



however these reactions still suffered heavily from issues in selectivity, overreactions, and polymerization.<sup>68, 71, 72</sup> Continual expansion of the field of fluorine chemistry led to the synthesis of N-fluorinated amines, which have an electrophilic fluorine contained in an N–F bond that is far less reactive than traditional electrophilic fluorinating reagents (BDE of F–F = 36 kcal/mol, BDE of selectfluor N–F bond = 64 kcal/mol) (**Figure 24**).<sup>73,74</sup>

With the arrival of electrophilic N–F reagents came with it the renaissance of fluorination chemistry.<sup>73</sup> Successful use of mild fluorine reagents lies in their relatively slow reaction rates. These new reagents allowed for reaction tuning by catalyst-ligand systems, paving the way for asymmetric fluorinations using a chiral catalyst. Differding and Lang achieved the first enantioselective fluorination in 1988 when they synthesized N-fluoro sultam, a chiral fluorinating reagent, which mediated the asymmetric fluorination of various prochiral metal enolates (**Figure 25**).<sup>74</sup> The setback of using stoichiometric chiral N–F reagent was having to still use F<sub>2</sub> gas along with multistep syntheses to prepare these enantioenriched N–F reagents, continuing the demand for new catalytic methods that could avoid demanding and dangerous reagent preparations.<sup>74-77</sup> With this in mind, the first transition metal-catalyzed enantioselective fluorination was demonstrated in 2000 when Tongi used a chiral Lewis acid titanium catalyst in combination with Selectfluor to asymmetrically  $\alpha$ -fluorinate activated  $\beta$ -carbonyl compounds.<sup>78</sup> Catalytic methods for electrophilic asymmetric fluorination chemistry rely on stoichiometric Selectfluor or NSF1 in pair with a transition metal catalyst, organocatalyst, or phase-transfer-catalyst to access to highly enantioenriched organofluorines.<sup>72, 77, 79</sup>

Differding and Lang 1988

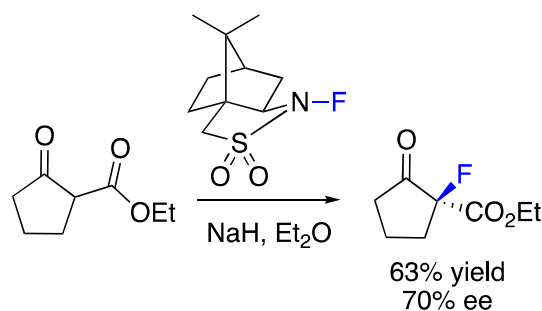
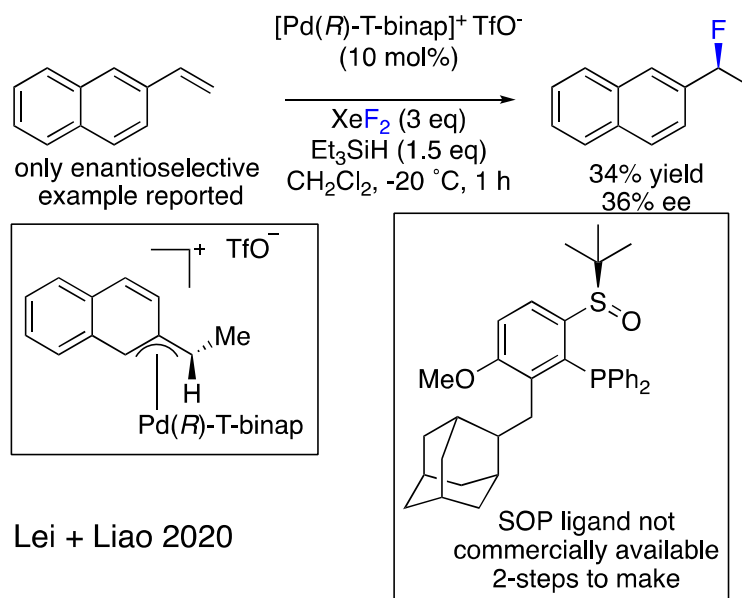


**Figure 25:** First Enantioselective Fluorination using a Chiral Fluorinating Reagent<sup>74</sup>

Currently, limitations in the chemoselectivity of fluorination reactions remain a frontier challenges in fluorination chemistry. Modern fluorination chemistry can be broken up into nucleophilic fluorinations, radical fluorinations, and electrophilic fluorinations. Compared to electrophilic fluorinations, significantly fewer nucleophilic and radical fluorination methodologies exist. Examples of enantioselective nucleophilic fluorinations are limited to ring openings of strained heterocycles and allylic substitutions.<sup>77, 80, 81</sup> Asymmetric radical fluorination methods are even more scarce and usually involve difunctionalization of an alkane with fluorine and another species, and these methods have relatively low ee and yields.<sup>82</sup> Asymmetric electrophilic fluorination is by far the most developed of the fluorination methods but has been fairly restricted to carbonyl compounds that can transform into metal enolates. Chiral amine catalysts have been employed to react with carbonyls *in situ* to form chiral enamine intermediates which can undergo asymmetric fluorination.<sup>77, 83, 84</sup> The dependency of electrophilic fluorinations on carbonyl compounds can be seen in the commercial fluorinated bioisosteres that contain a stereogenic C(sp<sup>3</sup>)–F bond, all of which are cyclic fluorinated compounds with limited structural diversity.<sup>60</sup>

## Gouverneur 2014



## Lei + Liao 2020

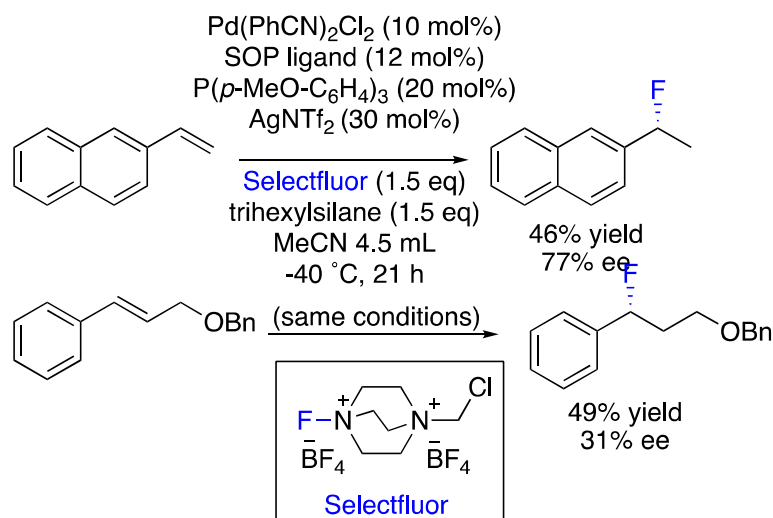


**Figure 26:** Previous Work and State-of-the-Art Enantioselective Transition Metal-Catalyzed Hydrofluorination of Alkenyl Arenes<sup>85, 87</sup>

Alkene hydrofluorination has emerged as a promising method for the enantioselective synthesis of organofluorines.<sup>85, 87</sup> Since the first addition of HF across an alkene<sup>66</sup>, several examples of metal-catalyzed regioselective additions of H and F across an alkene have been developed.<sup>72, 85-87</sup> In 2014 the Gouverneur group published a regioselective method for Pd-catalyzed hydrofluorination of alkenyl arenes.<sup>85</sup> This

method was accomplished by subjecting alkene substrates to a Pd precatalyst with stoichiometric Selectfluor as a fluorine source and Et<sub>3</sub>Si-H as a hydride source. In their investigation, chiral Pd-binap  $\pi$ -allyl complex (**Figure 26**) was formed with vinyl naphthalene using Hartwig's method<sup>88</sup> and it was observed that complex reacted with XeF<sub>2</sub> or Selectfluor to afford (*S*)-2-(1-fluoroethyl)naphthalene with 82% yield, 80% ee and 36% yield, 36% ee respectively (**Figure 26**). This was the first example of an asymmetric hydrofluorination of an alkene. The Lei and Liao group, as recently as 2020, has demonstrated a general protocol for enantioselective hydrofluorination of alkenyl arenes (**Figure 26**).<sup>87</sup>

### 2.3 Initial Results and Future Work

A variety of transition metal-catalyzed methods to fluorinate at the benzylic position of organic molecules have been reported. Benzylic C-H fluorination presents the opportunity for late-stage fluorination of complex molecules<sup>85, 87,89-95</sup> and alkene hydrofluorinations have been demonstrated to be highly regioselectivity.<sup>85-87</sup> Unfortunately, methods to synthesize organic molecules with benzylic C-F stereogenic centers with high enantioselectivity remain underdeveloped.<sup>85, 87</sup> State-of-the-art enantioselective hydrofluorinations cannot generate benzylic fluorine stereocenters that surpass 90% ee, averaging 76% ee across 26 examples (**Figure 26**). Examples of enantioselective hydrofluorinations of internal alkenyl arenes are severely limited and no examples have exceeded 31% ee (**Figure 26**).<sup>87</sup> The state-of-the-art method requires high loadings of precious metal precatalyst along and chiral ligand. Also, the chiral sulfoxide phosphine ligand employed in the catalytic transformation is not commercially available and requires some synthetic overhead.<sup>87</sup> An asymmetric precious metal-catalyzed directed

fluoroarylation of styrenes has also been reported. However, this method is an alkene difunctionalization and requires the use of a directing group.<sup>96</sup>

While more than half of the FDA approved fluorine-containing drugs in 2019 contain a stereocenter, less than 1% of these drugs contain a C-F stereocenter.<sup>58, 60</sup> Despite a clear demand for selective methods to fluorinate small molecules, no general synthetic methods are available for highly enantioselective hydrofluorination of alkenes. Our group believes that this constraint impedes the development of novel bioactive molecules with a fluorinated stereogenic center and inspired us to explore a Cu-catalyzed enantioselective hydrofluorination reaction for the synthesis of small molecules with chiral benzylic C(sp<sup>3</sup>)-F functionality.

Highly regio- and enantio- selective hydrofunctionalization of alkenyl arenes are possible using a chiral Cu-H catalyst.<sup>97</sup> Activated chiral Cu-H species are known to insert regioselectively into alkenes to form a benzylic copper intermediate, which is then subject to displacement in the presence of an electrophile. By employing an electrophilic fluorine source with a chiral Cu-H catalyst, we believe that successful benzylic fluorination is feasible. A bulky bidentate chiral ligand will serve to activate the Cu catalyst and provide sufficient enantioinduction to the reaction to achieve high ee.

Our preliminary data supports our hypothesis that a Cu-catalyzed enantioselective hydrofluorination of alkenyl arenes is possible. A Cu(OAc)<sub>2</sub> precatalyst in combination with bulky bidentate chiral (*S*)-DTBM SEGPPOS ligand were selected in combination with DMMS to form the active chiral Cu-H catalyst. We hypothesized that ethanol-OD, the electrophilic D-source used in our enantioselective transfer hydrodeuteration protocol (**Figure 27**) could be exchanged with an electrophilic fluorine source like Selectfluor to

enable a hydrofluorination process. Surprisingly, an unoptimized asymmetric hydrofluorination of 4-vinylbiphenyl provided the corresponding benzylic fluorine product **11** in 33% yield, with >20:1 regioselectivity and 84% ee, determined by chiral column HPLC (**Figure 27**).

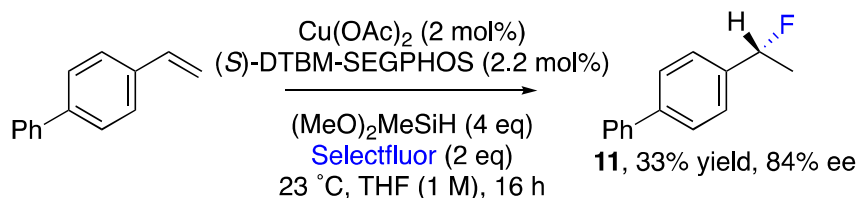


**Figure 27** Preliminary Results for Enantioselective Cu-Catalyzed Hydrofluorination

Mechanistically, this reaction is believed to operate very similarly to the transfer deuteration (**Figure 28**). The reaction initiates upon conversion of the  $\text{Cu}^{\text{II}}$  precatalyst to the active chiral Cu–H catalyst after transmetalation with DMMS. Regioselective hydrocupration of Cu–H into the alkenyl arene will form a resonance stabilized benzylic Cu intermediate that can undergo fluorodecupration in the presence of Selectfluor (or possibly another electrophilic fluorinating reagent) to give the product and a cationic Cu species which will regenerate the active Cu–H species after reaction with Si–H.

Selectfluor exhibits low solubility in many organic solvents and tends to only be soluble in polar solvents such as MeCN, DMF, and  $\text{H}_2\text{O}$  which are not compatible with the reductive conditions used in our proposed hydrofluorination reaction. It was reasoned that low reaction yields due to Selectfluor’s low solubility in THF could be investigated by using longer reaction times. When the reaction was run for 72 h instead of 16 h, yields improved up to 52%. Improvement of yield from 33% to 52% also occurred when the reaction was run 0.5 M in THF compared to 1 M used in the initial study. This is also indicative of a solubility issue with Selectfluor. Selectfluor’s poor solubility in organic

reagents is known.<sup>73, 74</sup> As a result, a variety of chiral anion phase transfer catalysts were developed during the renaissance of fluorination chemistry to overcome this issue.<sup>77</sup> Selectfluor with [OTf]<sup>-</sup> counter anions have been demonstrated to show superior solubility in organic solvents when compared with Selectfluor with [BF<sub>4</sub>]<sup>-</sup> counterions.<sup>74</sup> Substitution of the 2[BF<sub>4</sub>]<sup>-</sup> counterions on Selectfluor with 2[OTf]<sup>-</sup> counterions to investigate the effect of Selectfluor's solubility on reaction outcome (eq. (b), **Figure 29**).

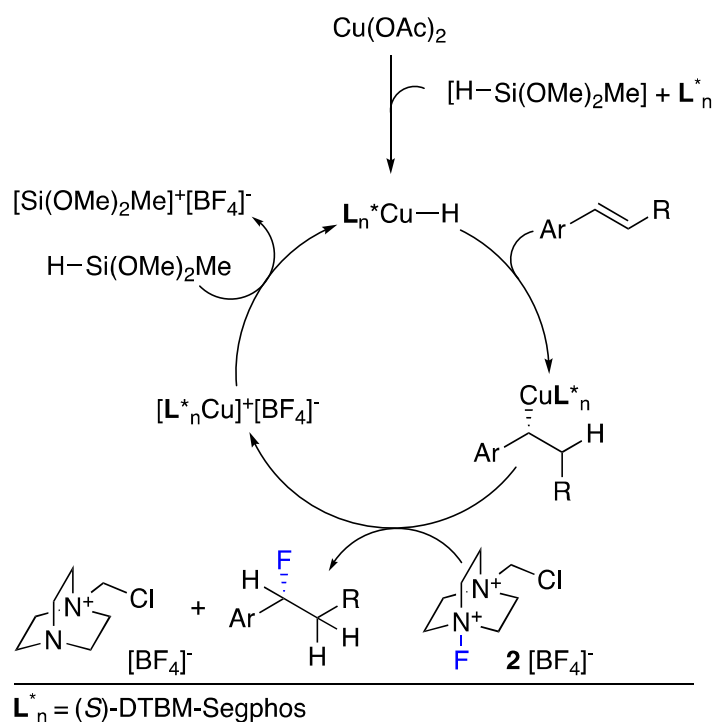


**Figure 28:** Proposed Mechanism for Enantioselective Cu-Catalyzed Hydrofluorination of Aryl Alkenes

Selectfluor contains two quaternary nitrogen atoms, one of which contains the N–F bond and the other can have a variety of alkyl or alkyl halide substitution. The most common alkyl substitution on the second quaternary nitrogen is methylene chloride (N–CH<sub>2</sub>Cl). Selectfluor is synthesized in five-steps from dabco (1,4-diazabicyclo[2.2.2]octane) (eq. (a), **Figure 29**).<sup>74</sup> By adjusting the synthetic route to adhere a more

lipophilic substituent such as an alkyl chain or a  $\text{CF}_3$  group to the nitrogen, both solubility and N–F bond strength can be adjusted (eq. (c), **Figure 29**). The N–F bond strength determines the reactivity of the fluorinating reagent. The weaker the bond, the more reactive the fluorinating reagent, and vice versa. When NSFI was substituted into the reaction, even at low temperatures, a variety of aryl fluorinated products were observed by  $^1\text{H-NMR}$  and  $^{19}\text{F-NMR}$ , with no benzylic fluorination observed. When N-fluoropyridinium was used, no reaction was observed and the starting alkenyl arene was completely recovered. According to literature, BDEs for N-fluoropyridinium, Selectfluor, and NFSI are 75.9 kcal/mol, 64.0 kcal/mol, and 63.4 kcal/mol respectively.<sup>75</sup> This puts Selectfluor's N–F bond strength lower than N-fluoropyridinium's and higher than NFSI's. Since N-fluoropyridinium showed no reactivity with the alkene and copper catalyst, the N–F bond is not reactive enough to fluorinate the benzylic copper intermediate. On the other hand, NFSI has a weaker N–F bond than Selectfluor, and did not yield fluorinated product, it did however, yield an aryl fluorination product, which could be due to a reactive radical intermediate. Since NFSI is highly soluble in organic solvent compared to Selectfluor, and has a lower BDE, it would make sense that both solubility and BDE of the fluorinating reagent play a significant role in the mechanistic pathway of this reaction.

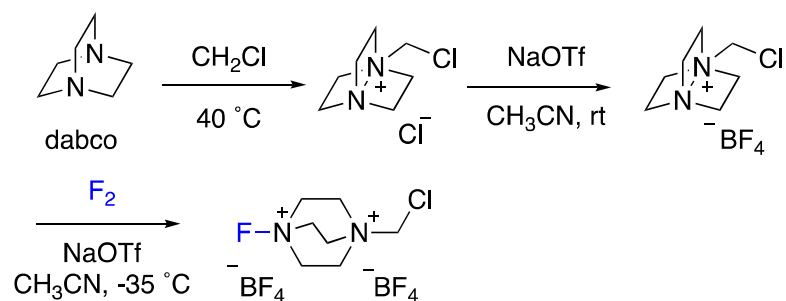
As mentioned previously, Selectfluor variants can be synthesized in five-steps from dabco (eq. (a), **Figure 29**).<sup>74</sup> Selectfluor's N–F BDE has been shown to decrease with increasing electron withdrawing substitution on the quaternary nitrogen. By synthesizing a series of Selectfluor derivatives with varying N–F bond strengths, the effect of N–F bond strength on product formation in the catalytic cycle can be examined



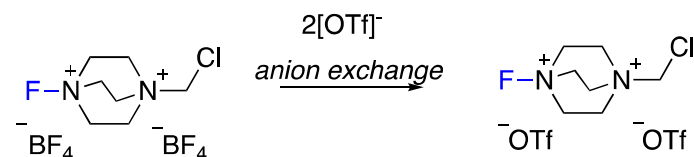
(eq. (c), **Figure 29**). When Selectfluor was used as the fluorinating reagent in the initial studies, significant quantities of starting material were recovered, which indicates insufficient reactivity associated with having ‘too strong’ of an N–F bond. By synthesizing Selectfluor derivatives with different alkyl or alkyl halide functionalities, the N–F BDE can be attenuated and its effect on the reaction outcome examined.

From our transfer hydrodeuteration optimization, we know that a variety of mixed solvent systems such as a 1,4-dioxane:THF mixture can enhance enantioselectivity. The Buchwald group has also found great success using THF, 1,4-dioxane, MTBE and mixed solvent systems in their enantioselective alkene hydrofunctionalizations.<sup>97, 98</sup> Additionally, we know that lowering the reaction temperature is also beneficial for achieving higher enantioselectivities in transfer hydrodeuteration. Full conversion of the alkene is not observed at room temperature using the current method, but once more reactive Selectfluor variants have been synthesized, running the reaction at 5 °C in a cold room may show improved enantioselectivity (eq. (c), **Figure 29**).

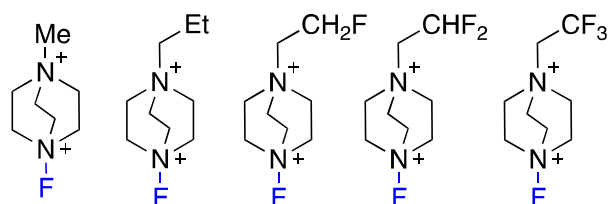
(a) synthesis of Selectfluor



(b) proposed anion exchange synthesis



(c) proposed Selectfluor derivatives

**Figure 29:** Synthesis of Selectfluor and Proposed Selectfluor Derivatives

Finally, electronically and sterically diverse alkenyl arene substrates will be examined (**Figure 30**). Electron neutral, electron donating, and electron withdrawing substituents will be analyzed first to determine the influence of aromatic substitution on the reaction. An *ortho*-substituted aromatic ring will provide insight into the degree of steric sensitivity of this reaction. Carbonyl groups have been known to undergo reductions under similar reductive catalytic conditions, the tolerance of the hydrofluorination to these groups will be explored. Internal alkenes have remained a challenge in hydrofluorination chemistry.<sup>87</sup> Both *Z*- and *E*- internal alkenes will be studied, along with a cyclic alkene, *2H*-chromene, to determine if alkene confirmation plays a role in reactivity. Finally, efficacy of the reaction will be tested on a quinoline

derivative. Since N-heterocyclic substrates showed substantial loss in ee in the transfer hydrodeuteration relative to the other heterocycles, I would like to compare the effect on ee of using an N-heterocyclic compound in the hydrofluorination reaction. If a marginal loss of ee is observed, then it may be fair to draw similarities between the hydrofluorination and hydrodeuteration mechanism.

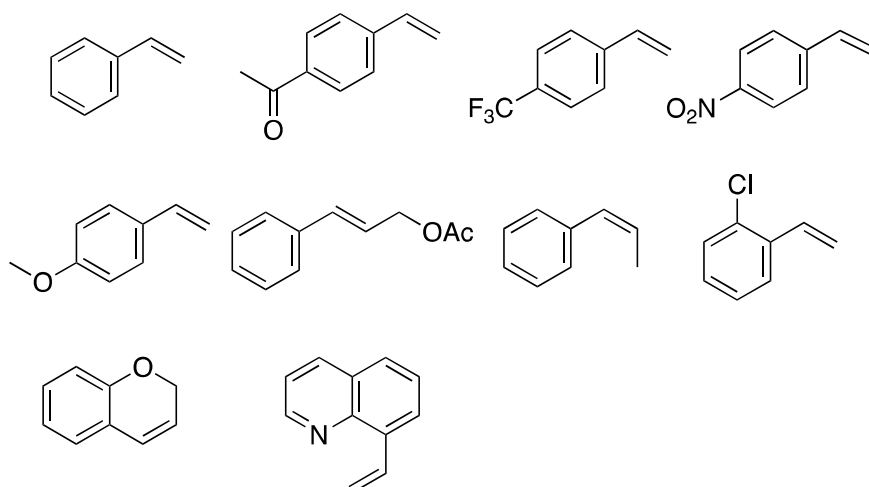


**Figure 30:** Initial Proposed Substrate Scope for the Hydrofluorination of Alkenyl Arenes

## BIBLIOGRAPHY

1. Urey, H. C.; Brickwedde, F. G.; Murphy, G. M., A Hydrogen Isotope of Mass 2 and its Concentration. *Physical Review* **1932**, *40* (1), 1-15.
2. Fu, I.; Woolf, E. J.; Matuszewski, B. K., Effect of the sample matrix on the determination of indinavir in human urine by HPLC with turbo ion spray tandem mass spectrometric detection. *Journal of Pharmaceutical and Biomedical Analysis* **1998**, *18* (3), 347-357.
3. Pirali, T.; Serafini, M.; Cargini, S.; Genazzani, A. A., Applications of Deuterium in Medicinal Chemistry. *Journal of Medicinal Chemistry* **2019**, *62* (11), 5276-5297.
4. Atzrodt, J.; Derdau, V.; Kerr, W. J.; Reid, M., C–H Functionalisation for Hydrogen Isotope Exchange. *Angewandte Chemie International Edition* **2018**, *57* (12), 3022-3047.
5. Atzrodt, J.; Derdau, V.; Kerr, W. J.; Reid, M., Deuterium- and Tritium-Labelled Compounds: Applications in the Life Sciences. *Angewandte Chemie International Edition* **2018**, *57* (7), 1758-1784.
6. Simmons, E. M.; Hartwig, J. F., On the Interpretation of Deuterium Kinetic Isotope Effects in C-H Bond Functionalizations by Transition-Metal Complexes. *Angewandte Chemie International Edition* **2012**, *51* (13), 3066-3072.
7. Giagou, T.; Meyer, M. P., Kinetic Isotope Effects in Asymmetric Reactions. *Chemistry – A European Journal* **2010**, *16* (35), 10616-10628.
8. Anslyn, E. V.; Dougherty, D. A., Modern physical organic chemistry. *University Science Books* **2006**.
9. Meek, S. J.; Pitman, C. L.; Miller, A. J. M., Deducing Reaction Mechanism: A Guide for Students, Researchers, and Instructors. *Journal of Chemical Education* **2016**, *93* (2), 275-286.
10. Schwab, J. M., Stereochemistry of an enzymic Baeyer-Villiger reaction. Application of deuterium NMR. *Journal of the American Chemical Society* **1981**, *103* (7), 1876-1878.
11. Leinberger, R.; Rétey, A.; Hull, W. E.; Simon, H., Steric Course of the NIH Shift in the Enzymic Formation of Homogentisic Acid. *European Journal of Biochemistry* **1981**, *117* (2), 311-318.

12. Battersby, A. R.; Gutman, A. L.; Fookes, C. J. R.; Günther, H.; Simon, H., Stereochemistry of formation of methyl and ethyl groups in bacteriochlorophyll a. *Journal of the Chemical Society, Chemical Communications* **1981**, (13), 645-647.
13. Lüthy, J.; Rétey, J.; Arigoni, D., Asymmetric Methyl Groups: Preparation and Detection of Chiral Methyl Groups. *Nature* **1969**, 221 (5187), 1213-1215.
14. Klinman, J. P., A new model for the origin of kinetic hydrogen isotope effects. *Journal of Physical Organic Chemistry* **2010**, 23 (7), 606-612.
15. White, R. E.; Miller, J. P.; Favreau, L. V.; Bhattacharyya, A., Stereochemical dynamics of aliphatic hydroxylation by cytochrome P-450. *Journal of the American Chemical Society* **1986**, 108 (19), 6024-6031.
16. Shapiro, S.; Piper, J. U.; Caspi, E., Steric course of hydroxylation at primary carbon atoms. Biosynthesis of 1-octanol from (1R)- and (1S)-[1-3H,2H,1H; 1-14C]octane by rat liver microsomes. *Journal of the American Chemical Society* **1982**, 104 (8), 2301-2305.
17. Jarling, R.; Sadeghi, M.; Drozdowska, M.; Lahme, S.; Buckel, W.; Rabus, R.; Widdel, F.; Golding, B. T.; Wilkes, H., Stereochemical Investigations Reveal the Mechanism of the Bacterial Activation of *n*-Alkanes without Oxygen. *Angewandte Chemie International Edition* **2012**, 51 (6), 1334-1338.
18. Chen, Y.; Tang, W. L.; Mou, J.; Li, Z., High-Throughput Method for Determining the Enantioselectivity of Enzyme-Catalyzed Hydroxylations Based on Mass Spectrometry. *Angewandte Chemie International Edition* **2010**, 49 (31), 5278-5283.
19. Groves, J. T.; Viski, P., Asymmetric hydroxylation by a chiral iron porphyrin. *Journal of the American Chemical Society* **1989**, 111 (22), 8537-8538.
20. Liu, W.; Cheng, M.-J.; Nielsen, R. J.; Goddard, W. A.; Groves, J. T., Probing the C–O Bond-Formation Step in Metalloporphyrin-Catalyzed C–H Oxygenation Reactions. *ACS Catalysis* **2017**, 7 (6), 4182-4188.
21. Morrison, J. D.; Tomaszewski, J. E.; Mosher, H. S.; Dale, J.; Miller, D.; Elsenbaumer, R. L., Hydrogen vs. deuterium transfer in asymmetric reductions: reduction of phenyl trifluoromethyl ketone by the chiral Grignard reagent from (*S*)-2-phenyl-1-bromoethane-1,1,2-d<sub>3</sub>. *Journal of the American Chemical Society* **1977**, 99 (9), 3167-3168.

22. Alberti, M. N.; Vassilikogiannakis, G.; Orfanopoulos, M., Stereochemistry of the Singlet Oxygenation of Simple Alkenes: A Stereospecific Transformation. *Organic Letters* **2008**, *10* (18), 3997-4000.
23. Curran, D. P.; Ramamoorthy, P. S., 1,2-Asymmetric induction in radical reactions. Deuteration and allylation reactions of  $\beta$ -oxy- $\alpha$ -bromo esters. *Tetrahedron* **1993**, *49* (22), 4841-4858.
24. Holcomb, H. L.; Nakanishi, S.; Flood, T. C., Stereochemistry at Carbon of the Cyclometalation of 8-( $\alpha$ -Deuterioethyl)quinoline by Palladium(II) Salts. *Organometallics* **1996**, *15* (20), 4228-4234.
25. Meanwell, N. A., Synopsis of Some Recent Tactical Application of Bioisosteres in Drug Design. *Journal of Medicinal Chemistry* **2011**, *54* (8), 2529-2591.
26. Harbeson, S. L.; Tung, R. D., Deuterium Medicinal Chemistry: A New Approach to Drug Discovery and Development. *Medchem News* **2014**, *24* (2), 8-22.
27. Gant, T. G., Using Deuterium in Drug Discovery: Leaving the Label in the Drug. *Journal of Medicinal Chemistry* **2014**, *57* (9), 3595-3611.
28. Nelson, S. D.; Trager, W. F., The Use of Deuterium Isotope Effects to Probe the active site properties, Mechanism of Cytochrom P450-Catalyzed Reactions, and Mechanisms of Metabolically Dependent Toxicity. *Drug Metabolism and Disposition* **2003**, *31* (12), 1481-1497.
29. Stepan, A. F.; Mascitti, V.; Beaumont, K.; Kalgutkar, A. S., Metabolism-guided drug design. *MedChemComm* **2013**, *4* (4), 631-652.
30. Schmidt, C., First deuterated drug approved. *Nature Biotechnology* **2017**, *35* (6), 493-494.
31. Dean, M.; Sung, V. W., Review of deutetrabenazine: a novel treatment for chorea associated with Huntington's disease. *Drug Design, Development and Therapy* **2018**, *12*, 313-319.
32. Atzrodt, J.; Derdau, V.; Fey, T.; Zimmermann, J., The Renaissance of H/D Exchange. *Angewandte Chemie International Edition* **2007**, *46* (41), 7744-7765.
33. Lee, S. H.; Gorelsky, S. I.; Nikonov, G. I., Catalytic H/D Exchange of Unactivated Aliphatic C-H Bonds. *Organometallics* **2013**, *32* (21), 6599-6604.

34. Neubert, L.; Michalik, D.; Bähn, S.; Imm, S.; Neumann, H.; Atzrodt, J.; Derdau, V.; Holla, W.; Beller, M., Ruthenium-Catalyzed Selective  $\alpha,\beta$ -Deuteration of Bioactive Amines. *Journal of the American Chemical Society* **2012**, *134* (29), 12239-12244.
35. Loh, Y. Y.; Nagao, K.; Hoover, A. J.; Hesk, D.; Rivera, N. R.; Colletti, S. L.; Davies, I. W.; MacMillan, D. W. C., Photoredox-catalyzed deuteration and tritiation of pharmaceutical compounds. *Science* **2017**, *358* (6367), 1182-1187.
36. Hale, L. V. A.; Szymczak, N. K., Stereoretentive Deuteration of  $\alpha$ -Chiral Amines with  $D_2O$ . *Journal of the American Chemical Society* **2016**, *138* (41), 13489-13492.
37. Palmer, W. N.; Chirik, P. J., Cobalt-Catalyzed Stereoretentive Hydrogen Isotope Exchange of  $C(sp^3)$ -H Bonds. *ACS Catalysis* **2017**, *7* (9), 5674-5678.
38. Esaki, H.; Aoki, F.; Umemura, M.; Kato, M.; Maegawa, T.; Monguchi, Y.; Sajiki, H., Efficient H/D Exchange Reactions of Alkyl-Substituted Benzene Derivatives by Means of the Pd/C-H<sub>2</sub>-D<sub>2</sub>O System. *Chemistry – A European Journal* **2007**, *13* (14), 4052-4063.
39. Atzrodt, J.; Derdau, V., Pd- and Pt-catalyzed H/D exchange methods and their application for internal MS standard preparation from a Sanofi-Aventis perspective. *Journal of Labelled Compounds and Radiopharmaceuticals* **2010**, *53* (11□12), 674-685.
40. Smith, J. A.; Wilson, K. B.; Sonstrom, R. E.; Kelleher, P. J.; Welch, K. D.; Pert, E. K.; Westendorff, K. S.; Dickie, D. A.; Wang, X.; Pate, B. H.; Harman, W. D., Preparation of cyclohexene isotopologues and stereoisotopomers from benzene. *Nature* **2020**, *581* (7808), 288-293.
41. Karlsson, S.; Hallberg, A.; Gronowitz, S., Hydrozirconation of (*E*)-3-methoxy-1-phenyl-1-propene and (*E*)-3-phenyl-2-propenol. *Journal of Organometallic Chemistry* **1991**, *403* (1), 133-144.
42. Walker, J. C. L.; Oestreich, M., Regioselective Transfer Hydrodeuteration of Alkenes with a Hydrogen Deuteride Surrogate Using  $B(C_6F_5)_3$  Catalysis. *Organic Letters* **2018**, *20* (20), 6411-6414.
43. Li, L.; Hilt, G., Regiodivergent DH or HD Addition to Alkenes: Deuterohydrogenation versus Hydrodeuterogenation. *Organic Letters* **2020**, *22* (4), 1628-1632.

44. Eliel, E. L., The Reduction of Optically Active Phenylmethylcarbonyl Chloride with Lithium Aluminum Deuteride. *Journal of the American Chemical Society* **1949**, *71* (12), 3970-3972.
45. Elsenbaumer, R. L.; Mosher, H. S., Enantiomerically pure (*R*)-(+)-2-phenylethanol-2-*d* and -1,1,2-*d*<sub>3</sub>, and (*S*)-(+)-1-phenylethane-1-*d*, -1,2-*d*<sub>2</sub>, -1,2,2-*d*<sub>3</sub>, and -1,2,2,2-*d*<sub>4</sub>. *The Journal of Organic Chemistry* **1979**, *44* (4), 600-604.
46. Küppers, J.; Rabus, R.; Wilkes, H.; Christoffers, J., Optically Active 1-Deuterio-1-phenylethane – Preparation and Proof of Enantiopurity. *European Journal of Organic Chemistry* **2019**, *2019* (15), 2629-2634.
47. Shi, S.; Buchwald, S. L., Copper-catalyzed Selective Hydroamination Reactions of Alkynes. *Nat. Chem.* **2015**, *7*, 38–44.
48. Liu, R. Y.; Buchwald, S. L., CuH-Catalyzed Olefin Functionalization: From Hydroamination to Carbonyl Addition. *Acc. Chem. Res.* **2020**, *53*, 1229–1243.
49. Wang, Y.; Huang, Z.; Leng, X.; Zhu, H.; Liu, G.; Huang, Z., Transfer Hydrogenation of Alkenes Using Ethanol Catalyzed by a NCP Pincer Iridium Complex: Scope and Mechanism. *J. Am. Chem. Soc.* **2018**, *140*, 4417–4429.
50. Sloane, S. E.; Reyes, A.; Vang, Z. P.; Li, L.; Behlow, K. T.; Clark, J. R., “Copper-Catalyzed Formal Transfer Hydrogenation/Deuteration of Aryl Alkynes” *Org. Lett.* **2020**, *22*, 9139-9144.
51. Neill, J. L.; Yang, Y.; Muckle, M. T.; Reynolds, R. L.; Evangelisti, L.; Sonstrom, R. E.; Pate, B. H.; Gupton, B. F., Online Stereochemical Process Monitoring by Molecular Rotational Resonance Spectroscopy. *Organic Process Research & Development* **2019**, *23* (5), 1046-1051.
52. Pate, B.H.; Evangelisti, L.; Caminati, W.; Xu, Y.; Thomas, J.; Patterson, D.; Perez, C.; Schnell, M., Quantitative chiral analysis by molecular rotational spectroscopy. In *Chiral Analysis: Advances in Spectroscopy, Chromatography, and Emerging Methods*, 2 ed.; Polavarapu, P., Ed. Elsevier: 2018.



53. Joyce, L. A.; Schultz, Danielle M.; Sherer, E. C.; Neill, J. L.; Sonstrom, R. E.; Pate, B. H., Direct regioisomer analysis of crude reaction mixtures via molecular rotational resonance (MRR) spectroscopy. *Chemical Science* **2020**, *11* (24), 6332-6338.
54. Neill, J. L.; Mikhonin, A. V.; Chen, T.; Sonstrom, R. E.; Pate, B. H., Rapid quantification of isomeric and dehalogenated impurities in pharmaceutical raw materials using MRR spectroscopy. *Journal of Pharmaceutical and Biomedical Analysis* **2020**, *189*, 113474.
55. Brown, G.G.; Dian, B.C.; Douglass, K.O.; Geyer, S.M.; Pate, B.H., A Broadband Fourier Transform Microwave Spectrometer Based on Chirped Pulse Excitation. *Rev. Sci. Instrum.* **2008**, *79*, 053103.
56. Grimme, S.; Steinmetz, M., Effects of London dispersion correction in density functional theory on the structures of organic molecules in the gas phase. *Physical Chemistry Chemical Physics* **2013**, *15* (38), 16031-16042.
57. Wang, J.; Sánchez-Roselló, M.; Aceña, J. L.; del Pozo, C.; Sorochinsky, A. E.; Fustero, S.; Soloshonok, V. A.; Liu, H., Fluorine in Pharmaceutical Industry: Fluorine-Containing Drugs Introduced to the Market in the Last Decade (2001–2011). *Chemical Reviews* **2014**, *114* (4), 2432-2506.
58. Inoue, M.; Sumii, Y.; Shibata, N., Contribution of Organofluorine Compounds to Pharmaceuticals. *ACS Omega* **2020**, *5* (19), 10633-10640.
59. Mei, H.; Remete, A. M.; Zou, Y.; Moriwaki, H.; Fustero, S.; Kiss, L.; Soloshonok, V. A.; Han, J., Fluorine-containing drugs approved by the FDA in 2019. *Chinese Chemical Letters* **2020**, *31* (9), 2401-2413.
60. Mei, H.; Han, J.; Fustero, S.; Medio-Simon, M.; Sedgwick, D. M.; Santi, C.; Ruzziconi, R.; Soloshonok, V. A., Fluorine-Containing Drugs Approved by the FDA in 2018. *Chemistry – A European Journal* **2019**, *25* (51), 11797-11819.
61. Zhu, Y.; Han, J.; Wang, J.; Shibata, N.; Sodeoka, M.; Soloshonok, V. A.; Coelho, J. A. S.; Toste, F. D., Modern Approaches for Asymmetric Construction of Carbon–Fluorine Quaternary Stereogenic Centers: Synthetic Challenges and Pharmaceutical Needs. *Chemical Reviews* **2018**, *118* (7), 3887-3964.
62. Dong, C.; Huang, F.; Deng, H.; Schaffrath, C.; Spencer, J. B.; O'Hagan, D.; Naismith, J. H., Crystal Structure and Mechanism of a Bacterial Fluorinating Enzyme. *Nature* **2004**, *427*, 561-565.

63. O'Hagan, D.; Schaffrath, C.; Cobb, S. L.; Hamilton, J. T.; Murphy, C. D., Biochemistry: Biosynthesis of an Organofluorine Molecule. *Nature* **2002**, *416*, 279-280.
64. Littlechild, J., Haloperoxidases and their role in biotransformation reactions. *Curr. Opin. Chem. Biol.* **1999**, *3*, 28–34.
65. vanPee, K.H., Biosynthesis of halogenated metabolites by bacteria. *Annu. Rev. Microbiol.* **1996**, *50*, 375–399.
66. Grosse, A.V.; Linn, C.B., The Addition of Hydrogen Fluoride to the Double Bond. *J. Org. Chem.* **1938**, *03*, 1, 26–32.
67. Okazoe, T., Overview on the history of organofluorine chemistry from the viewpoint of material industry *Proc. Jpn. Acad. Ser. B Phys. Biol. Sci.* **2009**, *85*, 276-289.
68. Banks, R.E.; Tatlow, J.C., Synthesis of C-F bonds: the pioneering years, 1835-1940. *J. Fluorine Chem.* **1986**, *33*, 71-108.
69. Moissan, H., Action d'un Courant Électrique sur l'Acide Fluorhydrique Anhydre, *Compt. Rend.*, **1886**, *102*, 1543-1544.
70. Merritt, R. F., Direct Fluorination of 1,1-Diphenylethylene. *J. Org. Chem.* **1966**, *31*, 3871.
71. Rozen, S., Selective Fluorinations by Reagents Containing the OF Group. *Chem. Rev.*, **1996**, *96*, 1717–1736.
72. Bertrand, X.; Chabaud, L.; Paquin, J.-F., Hydrofluorination of Alkenes: A Review *Chem Asian J.* **2021**, *16*, 563 –574.
73. Ronald, E.B., Selectfluor<sup>TM</sup> reagent F-TEDA-BF<sub>4</sub>, in action: tamed fluorine at your service *Journal of Fluorine Chemistry* **1998**, *87*, 1-17.
74. Differding, E.; Land, R.W., New Fluorinating Reagents – I. The First Enantioselective Fluorination Reaction. *Tetrahedron Letters*, **1988**, *29*, 6087-6090.
75. Yang, J.-D.; Wang, Y.; Xue, X.-S.; Cheng, J.-P., A Systematic Evaluation of the N–F Bond Strength of Electrophilic N–F Reagents: Hints for Atomic Fluorine Donating Ability *J. Org. Chem.* **2017**, *82*, 4129–4135.
76. Nyffeler, P.T.; Durón, S.G.; Burkart, M.D.; Vincent, S.P.; Wong, C.-H., Selectfluor: Mechanistic Insight and Applications. *Angew. Chem. Int. Ed.* **2005**, *44*, 192 – 212.

77. Thornbury, R.; Schäfer, G.; Toste, F.D., 9 - Catalytic Enantioselective Fluorination. In *Modern Synthesis Processes and Reactivity of Fluorinated Compounds*, 1 ed.; Groult, H.; Leroux, F.; Tressaud, A., Ed. Elsevier: 2016.
78. Hintermann, L.; Togni, A. Catalytic Enantioselective Fluorination of  $\beta$ -Ketoesters. *Angew. Chem. Int. Ed.* **2000**, *39*, 4359-4362.
79. Cahard, D.; Xu, X.; Couve-Bonnaire, S.; Pannecoucke, X., Fluorine & chirality: how to create a nonracemic stereogenic carbon-fluorine centre? *Chem. Soc. Rev.*, **2010**, *39*, 558–568.
80. Kalow, J.A.; Doyle, A.G. Enantioselective Ring Opening of Epoxides by Fluoride Anion Promoted by Dual-catalyst System. *J. Am. Chem. Soc.* **2010**, *132*, 3268-3269.
81. Katcher, M.H.; Doyle, A.G. Palladium-catalyzed Asymmetric Synthesis of Allylic Fluorides. *J. Am. Chem. Soc.* **2010**, *132*, 17402-17404.
82. Chen, C.; Fu, L.; Chen, P.; Liu, G., Recent Advances and Perspectives of Transition Metal-Catalyzed Asymmetric Fluorination Reactions. *Chin. J. Chem.* **2017**, *35*, 1781—1788.
83. Kwiatkowski, P.; Beeson, T. D.; Conrad, J. C.; Macmillan, D. W. Enantioselective Organocatalytic Alpha-fluorination of Cyclic Ketones. *J. Am. Chem. Soc.* **2011**, *133*, 1738-1741.
84. Lam, Y. H.; Houk, K. N. How Cinchona Alkaloid-derived Primary Amines Control Asymmetric Electrophilic Fluorination of Cyclic Ketones. *J. Am. Chem. Soc.* **2014**, *136*, 9556-9559.
85. Emer, E.; Pfeifer, L.; Brown, J. M.; Gouverneur, V., *cis*-Specific Hydrofluorination of Alkenylarenes under Palladium Catalysis through an Ionic Pathway. *Angewandte Chemie International Edition* **2014**, *53* (16), 4181-4185.
86. Barker, T. J.; Boger, D. L., Fe(III)/NaBH<sub>4</sub>-Mediated Free Radical Hydrofluorination of Unactivated Alkenes. *Journal of the American Chemical Society* **2012**, *134* (33), 13588-13591.
87. Yin, X.; Chen, B.; Qiu, F.; Wang, X.; Liao, Y.; Wang, M.; Lei, X.; Liao, J., Enantioselective Palladium-Catalyzed Hydrofluorination of Alkenylarenes. *ACS Catalysis* **2020**, *10* (3), 1954-1960.

88. Nettekoven, U.; Hartwig, J.F., A New Pathway for Hydroamination. Mechanism of Palladium-Catalyzed Addition of Anilines to Vinylarenes. *J. Am. Chem. Soc.*, **2002**, *124*, 1166-1167.
89. Liu, W.; Groves, J. T., Manganese Catalyzed C–H Halogenation. *Accounts of Chemical Research* **2015**, *48* (6), 1727-1735.
90. Bloom, S.; Pitts, C. R.; Woltornist, R.; Griswold, A.; Holl, M. G.; Lectka, T., Iron(II)-Catalyzed Benzylic Fluorination. *Organic Letters* **2013**, *15* (7), 1722-1724.
91. Cantillo, D.; de Frutos, O.; Rincón, J. A.; Mateos, C.; Kappe, C. O., A Continuous-Flow Protocol for Light-Induced Benzylic Fluorinations. *The Journal of Organic Chemistry* **2014**, *79* (17), 8486-8490.
92. Bloom, S.; Pitts, C. R.; Miller, D. C.; Haselton, N.; Holl, M. G.; Urheim, E.; Lectka, T., A Polycomponent Metal-Catalyzed Aliphatic, Allylic, and Benzylic Fluorination. *Angewandte Chemie International Edition* **2012**, *51* (42), 10580-10583.
93. Groendyke, B. J.; AbuSalim, D. I.; Cook, S. P., Iron-Catalyzed, Fluoroamide-Directed C–H Fluorination. *Journal of the American Chemical Society* **2016**, *138* (39), 12771-12774.
94. Hua, A. M.; Mai, D. N.; Martinez, R.; Baxter, R. D., Radical C–H Fluorination Using Unprotected Amino Acids as Radical Precursors. *Organic Letters* **2017**, *19* (11), 2949-2952.
95. Nodwell, M. B.; Bagai, A.; Halperin, S. D.; Martin, R. E.; Knust, H.; Britton, R., Direct photocatalytic fluorination of benzylic C–H bonds with N-fluorobenzenesulfonimide. *Chemical Communications* **2015**, *51* (59), 11783-11786.
96. Talbot, E. P. A.; Fernandes, T. d. A.; McKenna, J. M.; Toste, F. D., Asymmetric Palladium-Catalyzed Directed Intermolecular Fluoroarylation of Styrenes. *Journal of the American Chemical Society* **2014**, *136* (11), 4101-4104.
97. Zhu, S.; Niljianskul, N.; Buchwald, S.L., Enantio- and Regioselective CuH-Catalyzed Hydroamination of Alkenes. *J. Am. Chem. Soc.* **2013**, *135*, 15746–15749.
98. Liu, R.Y.; Zhou, Y.; Yang, Y.; Buchwald, S.L., Enantioselective Allylation Using Allene, a Petroleum Cracking Byproduct. *J. Am. Chem. Soc.*, **2019**, *141*, 2251-2256.

## METHODS AND MATERIALS

**I. General Information**

The following chemicals were purchased from commercial vendors and were used as received:

(*R*)-(-)-Methyl Mandelate (Oakwood Chemicals); Lithium Aluminum Hydride (LiAlH<sub>4</sub>) (Acros Organics); Lithium Aluminum Deuteride (LiAlD<sub>4</sub>) (Boc Sciences); Dimethoxyethane (Oakwood Chemicals); 2,2-dimethoxypropane (Oakwood Chemicals); 1,1,1-trimethoxyethane (Oakwood Chemicals); N-Fluoro-N'-chloromethyltriethylenediamine bis(tetrafluoroborate) (Oakwood Chemicals); Trimethylsilyl Chloride (Alfa Aesar); (*S*)-1-Phenylethanol (Ambeed Inc.); 1-Formalpyrrolidine (Oakwood Chemicals); Tosyl chloride (Oakwood Chemicals); Benzoyl chloride (Avocado Research Chemicals Ltd.); Cu(OAc)<sub>2</sub> (99.999% from Alfa Aesar); Dimethoxy(methyl)silane (TCI); Ethanol-OD (Millipore Sigma); Poly(methylhydrosiloxane) average M<sub>n</sub> 1700-3200 (Millipore Sigma);

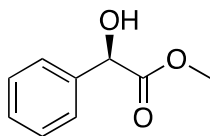
Anhydrous tetrahydrofuran (THF) and diethyl ether (Et<sub>2</sub>O) were purified by an MBRAUN solvent purification system (MB-SPS). Dimethoxyethane (DME) and Chloroform-*d* (CDCl<sub>3</sub>) were stored over 3Å molecular sieves. Thin-layer chromatography (TLC) was conducted with Silicycle silica gel 60Å F254 pre-coated plates (0.25 mm) and visualized with UV and a KMnO<sub>4</sub> stain. Flash chromatography was performed using SiliaFlash® P60, 40-60 mm (230-400 mesh), purchased from Silicycle. For reactions that required heating (optimization, transfer hydrodeuteration), a PolyBlock for 5-dram vials was used on top of a Heidolph heating/stir plate.

<sup>1</sup>H NMR spectra were recorded on a Varian 300 or 400 MHz spectrometer and are reported in ppm using deuterated solvent as an internal standard (CDCl<sub>3</sub> at 7.26 ppm). Data reported as: s = singlet, d = doublet, t = triplet, q = quartet, p = pentet, sxt = sextet, m = multiplet, br = broad; coupling constant(s) in Hz; integration. <sup>13</sup>C NMR spectra were recorded on a Varian 76 MHz or 101 MHz spectrometer and are reported in ppm using deuterated solvent as an internal standard (CDCl<sub>3</sub> at 77.16 ppm). <sup>2</sup>H NMR spectra were recorded on a Varian 61 MHz spectrometer. <sup>19</sup>F NMR spectra were recorded on a Varian (376 MHz) spectrometer and are reported in ppm using solvent as an internal standard (CDCl<sub>3</sub>). Chiral high pressure liquid chromatography (HPLC) analysis was performed on a Shimadzu LC-20AT instrument equipped with a SPD-20A UV detector, using a Phenomenex Lux<sup>®</sup> 5 μm Cellulose-3 column.

High-resolution mass spectra were obtained for all new compounds not previously reported using the resources of the Chemistry Instrument Center (CIC), University at Buffalo, SUNY, Buffalo, NY. Specifically, high resolution accurate mass analysis was conducted using the following instruments: 12T Bruker SolarixR 12 Hybrid FTMS with Imaging MALDI and Nano-LC, provided through funding from the National Institutes of Health, NIH S10 RR029517; a Thermo Q-Exactive Focus Orbitrap Liquid Chromatograph Tandem Mass Spectrometer and a Thermo Q-Exactive Orbitrap Gas Chromatograph Tandem Mass Spectrometer, provided through funding from the National Science Foundation, MRI-1919594.

Method verification and development of experimental protocol for deuterated compounds via molecular rotational resonance (MRR) were obtained using an off-line 2-8 GHz broadband MRR spectrometer at the University of Virginia (UVA), Charlottesville, VA. Reaction optimization for deuteration was performed using a cavity-enhanced MRR spectrometer at BrightSpec INC, Charlottesville, VA.

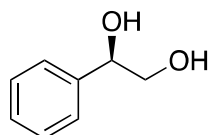
## I. Mosher's Synthesis



**(R)-(-)-Methyl Mandelate [13].** To a 300 mL round bottom flask was added (*R*)-mandelic acid (30 g, 0.20 mol, 1.0 eq.), MeOH (15 mL, 0.26 mol, 1.3 eq.), and 2,2-dimethoxypropane (24 mL, 0.20 mol, 1.0 eq.), followed by concentrated H<sub>2</sub>SO<sub>4</sub> (1.5 mL). The reaction mixture was refluxed for 4 h and then concentrated under reduced pressure. The resulting dark brown oil was recrystallized from hexane (750 mL) to give (*R*)-(-)-methyl mandelate as a white solid (20 g, 0.12 mol, 61% yield). The NMR data was consistent with previously reported spectra.<sup>1</sup>

<sup>1</sup>H NMR: (400 MHz, CDCl<sub>3</sub>)

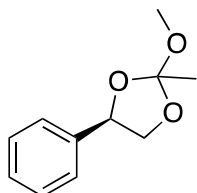
δ 7.44 – 7.31 (m, 5H), 5.18 (s, 1H), 3.77 (s, 3H), 3.04 (br s, 1H).



**(R)-(-)-Phenylethylene Glycol [14].** To a flame-dried 500 mL Schlenk tube under a N<sub>2</sub> atmosphere was added a solution of LiAlH<sub>4</sub> (1.8 g, 47 mmol 1.1 eq.) in DME (15 mL) followed by a slow addition of (*R*)-(-)-methyl mandelate (7.4 g, 45 mmol, 1.0 eq.) in DME (100 mL). The mixture was stirred for 12 h at 23 °C and hydrolyzed with saturated aqueous NH<sub>4</sub>Cl (10 mL) followed by HCl (20 mL, 2 M). The DME layer was set aside, and the aqueous layer was extracted with Et<sub>2</sub>O (3 x 20 mL). HCl (2 M) was added to the aqueous layer until the salts were completely dissolved and the aqueous layer was extracted with ether Et<sub>2</sub>O (3 x 20 mL). The combined organic layers were dried with Na<sub>2</sub>SO<sub>4</sub> and concentrated under reduced pressure. The resulting crude mixture was recrystallized in benzene/hexane (30 mL, 3:1) to give (*R*)-(-)-phenylethylene glycol as a white solid (5.5 g, 40 mmol, 89% yield). The NMR data was consistent with previously reported spectra.<sup>1</sup>

$^1\text{H NMR}$ : (400 MHz,  $\text{CDCl}_3$ )

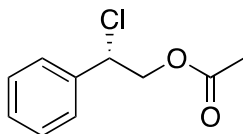
$\delta$  7.38 – 7.34 (m, 4H), 7.34 – 7.28 (m, 1H), 4.85 – 4.79 (m, 1H), 3.79 – 3.72 (m, 1H), 3.70 – 3.62 (m, 1H), 2.76 – 2.71 (m, 1H), 2.34 – 2.26 (m, 1H).



**(2 *RS*, 4 *R*)-2-Methoxy-2-methyl-4-phenyl-1,3-dioxolane [15]**. A mixture of (*R*)-(-)-phenylethylene glycol (2.0 g, 14 mmol, 1.0 eq.), 1,1,1-trimethoxyethane (4.80 mL, 36.4 mmol, 2.6 eq.) and concentrated  $\text{H}_2\text{SO}_4$  (30  $\mu\text{L}$ ) was stirred in a 50 mL round bottom flask at 23  $^\circ\text{C}$  for 10 min followed by heating at 50  $^\circ\text{C}$  for 1 h under reduced pressure. The residual red oil was dry loaded onto a silica gel column and purified by flash column chromatography (200 mL of 10% EtOAc in hexanes) to give diastereomers (2 *RS*, 4 *R*)-2-methoxy-2-methyl-4-phenyl-1,3-dioxolane as a red oil (1.02 g, 5.30 mmol, 36% yield). The NMR data was consistent with previously reported spectra.<sup>1</sup>

$^1\text{H NMR}$ : (400 MHz,  $\text{CDCl}_3$ )

$\delta$  7.46 – 7.27 (m, 5H), 5.25 (t,  $J = 7.2$  Hz, 0.6H), 5.13 (dd,  $J = 9.6, 6.5$  Hz, 0.38H), 4.46 (dd,  $J = 8.0, 6.9$  Hz, 0.64H), 4.33 (dd,  $J = 8.0, 6.5$  Hz, 0.41H), 3.86 (dd,  $J = 9.6, 8.0$  Hz, 0.40H), 3.78 (t,  $J = 7.8$  Hz, 0.64H), 3.42 (s, 1.13H), 3.38 (s,  $J = 0.6$  Hz, 1.81H), 1.71 (s, 1.91H), 1.66 (s, 1.18H).



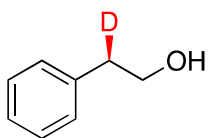
**(*S*)-(-)-2-Chloro-2-Phenethyl Acetate [16]**. To a flame-dried 25 mL Schlenk tube under a  $\text{N}_2$  atmosphere was added a solution of (2 *RS*, 4 *R*)-2-methoxy-2-methyl-4-phenyl-1,3-dioxolane (800 mg, 4.12 mmol, 1.0 eq.) in DCM (2 mL) at 0  $^\circ\text{C}$  followed by trimethylsilyl chloride (1.56 mL, 12.3 mmol, 3.0 eq.). After stirring for 2 h at 0  $^\circ\text{C}$  the



mixture was concentrated under reduced pressure. The residual beige oil was dry loaded onto a silica gel column and purified by flash column chromatography (200 mL of 10% EtOAc in hexanes) to give (*S*)-(-)-2-chloro-2-phenethyl acetate as a light brown oil (650 mg, 3.3 mmol, 79% yield). The NMR data was consistent with previously reported spectra.<sup>1</sup>

<sup>1</sup>H NMR: (400 MHz, CDCl<sub>3</sub>)

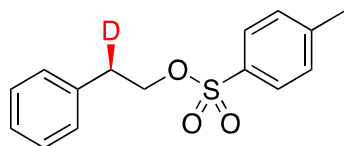
δ 7.44 – 7.34 (m, 5H), 5.07 (t, *J* = 7.14, 6.53, 1H), 4.52 – 4.39 (m, 2H), 2.07 (s, 3H).



**(*R*)-(+)-2-Phenylethanol-2-*d*<sub>1</sub> [17].** A suspension of LiAlD<sub>4</sub> (159 mg, 3.8 mmol, 1.25 eq.) in DME (7 mL) was stirred under N<sub>2</sub> at 23 °C for 30 min in a flame-dried 25 mL Schlenk tube followed by a slow addition of (*S*)-(-)-2-chloro-2-phenethyl acetate (650 mg, 3.3 mmol, 1.0 eq.) in DME (2.5 mL). After stirring for 7 h at 23 °C, the mixture was hydrolyzed with saturated aqueous NH<sub>4</sub>Cl (5 mL) and then HCl (5 mL, 2 M). The DME layer was set aside, and the aqueous layer was extracted with Et<sub>2</sub>O (3 x 10 mL). HCl (2 M) was added to the aqueous layer until the salts were completely dissolved and the aqueous layer was extracted with Et<sub>2</sub>O (3 x 10 mL). The combined organic layers were dried over Na<sub>2</sub>SO<sub>4</sub> and concentrated under reduced pressure. The resulting yellow oil was dry loaded onto a silica gel column and purified by gradient flash column chromatography (100 mL of 10% EtOAc in hexanes, 200 mL of 20% EtOAc in hexanes) to give (*R*)-(+)-2-phenylethanol-2-*d*<sub>1</sub> as a light-yellow oil (384 mg, 3.12 mmol, 95% yield). The NMR data was consistent with previously reported spectra.<sup>1</sup>

<sup>1</sup>H NMR: (400 MHz, CDCl<sub>3</sub>)

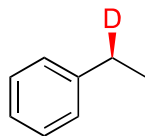
δ 7.39 – 7.29 (m, 2H), 7.29 – 7.20 (m, 3H), 3.91 – 3.79 (m, 2H), 2.92 – 2.81 (m, 1H), 1.56 (br s, 1H).



**(R)-(+)-2-Phenylethyl-2- $d_1$ -tosylate [18].** To a flame-dried 25 mL Schlenk tube under a  $N_2$  atmosphere was added (*R*)-(+)-2-phenylethanol-2- $d_1$  (384 mg, 3.1 mmol, 1.0 eq.) and pyridine (3.8 mL) and cooled on an ice bath followed by slow addition of toluenesulfonyl chloride (663 mg, 3.5 mmol, 1.2 eq.). After stirring at 23 °C for 1 h, the reaction vessel was placed in the refrigerator overnight. The reaction mixture was poured onto ice water and extracted with  $Et_2O$  (4 x 15 mL). The combined organic layers were washed with aqueous 10 %  $H_2SO_4$  (15 mL) solution followed by saturated aqueous  $NaHCO_3$  (15 mL) and then dried over  $Na_2SO_4$ . The combined organic layers were concentrated under reduced pressure, dry loaded onto a silica gel column and purified by gradient flash column chromatography (100 mL hexanes, 100 mL of 5 %  $Et_2O$  in hexanes, 100 mL of 10 %  $Et_2O$  in hexanes, 100 mL of 15%  $Et_2O$  in hexanes) to yield (*R*)-(+)-2-phenylethyl-2- $d_1$ -tosylate as a light-yellow solid (444 mg, 1.60 mmol, 51% yield). The NMR data was consistent with previously reported spectra.<sup>1</sup>

$^1H$  NMR: (400 MHz,  $CDCl_3$ )

$\delta$  7.69 (d,  $J = 8.1$  Hz, 2H), 7.31 – 7.19 (m, 5H), 7.12 (d, 2H), 4.20 (d,  $J = 7.1$  Hz, 2H), 2.99 – 2.89 (m, 1H), 2.43 (s, 3H).

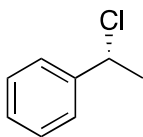


**(S)-(+)-1-Phenylethane-1- $d_1$  [2].** To a flame-dried 10 mL round bottom flask under a  $N_2$  atmosphere was added  $LiAlH_4$  (97 mg, 2.6 mmol, 1.6 eq.) and tetraglyme (3 mL). The flask was evacuated with stirring to remove any volatile impurities. Upon refilling the flask with  $N_2$ , (*R*)-(+)-2-phenylethanol-2- $d_1$  (444 mg, 1.60 mmol, 1.0 eq.) was added and the flask was re-evacuated. The flask was fitted with a distillation head and heated at 60 °C under vacuum to give (*S*)-(+)-1-Phenylethane-1- $d_1$  in a cold trap (34 mg, 0.32 mmol, 20% yield). The NMR data was consistent with previously reported spectra.<sup>1</sup>

$^1\text{H NMR}$ : (400 MHz,  $\text{CDCl}_3$ )

$\delta$  7.30 (t,  $J = 7.5$  Hz, 2H), 7.25 – 7.16 (m, 3H), 2.71 – 2.60 (m, 1H), 1.29 – 1.22 (m, 3H).

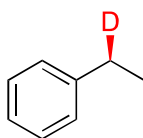
## II. Christoffers' Synthesis



**(*R*)-(1-Chloroethyl)benzene [19]**. To a flame-dried 100 mL Schlenk tube under a  $\text{N}_2$  atmosphere was added (*S*)-1-phenylethanol (2.44 g, 20.0 mmol, 1.0 eq.) and 1-formylpyrrolidine (0.4 mL, 4 mmol, 0.2 eq.). The mixture was cooled to  $0^\circ\text{C}$  and benzoyl chloride (3.5 mL, 30 mmol, 1.5 eq.) was added slowly over 5 min and the reaction was stirred at  $0^\circ\text{C}$  for 2 h, then at  $23^\circ\text{C}$  for 24 h. After 24 h, Ethanolamine (2.44 g, 40.0 mmol, 2.0 eq.) was added, and the mixture was stirred at  $23^\circ\text{C}$  for 30 min. The reaction was diluted with  $\text{Et}_2\text{O}$  (60 mL) and cooled on an ice bath. Saturated aqueous  $\text{NaHCO}_3$  (20 mL) and water (10 mL) were added, and the mixture was stirred for 5 min at  $0^\circ\text{C}$ . The layers were separated, and the organic layer was washed with saturated aqueous  $\text{NaHCO}_3$  (20 mL) and dried over  $\text{Na}_2\text{SO}_4$ . The mixture was filtered, and the solvent was removed by rotary evaporation. The resulting crude oil was dry loaded onto a silica gel column and purified by flash column chromatography (300 mL of 0.5%  $\text{Et}_2\text{O}$  in *n*-pentane) to give (*R*)-(1-chloroethyl)benzene as a clear colorless oil (1.55 g, 11.0 mmol, 55 %). The NMR data was consistent with previously reported spectra.<sup>2</sup>

$^1\text{H NMR}$ : (400 MHz,  $\text{CDCl}_3$ )

$\delta$  7.46 – 7.41 (m, 2H), 7.37 (tt,  $J = 6.4, 1.0$  Hz, 2H), 7.33 – 7.28 (m, 1H), 5.10 (q,  $J = 6.8$  Hz, 1H), 1.86 (d,  $J = 6.8$  Hz, 3H). °

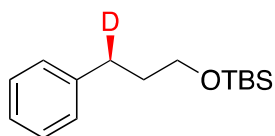


**(S)-(+)-1-Phenylethane-1-*d*<sub>1</sub> [2]**. To a flame-dried 250 mL round bottom flask under a N<sub>2</sub> atmosphere was added (*R*)-(1-chloroethyl)benzene (1.55 g, 11.0 mmol, 1.0 eq.) and THF (82 mL). The reaction was cooled on an ice bath and LiAlD<sub>4</sub> (927 mg, 22.0 mmol, 2.0 eq.) was quickly added to the mixture and the reaction vessel was fitted with a condenser and stirred at 75 °C for 20 h. The heat was removed, and the reaction was cooled on an ice bath and diluted with ice-cold water (10 mL). The aqueous layer was extracted with *n*-pentane (3 x 10 mL) and the combined organic layers were washed in the following sequence using phosphoric acid (85%, 30 mL), water (30 mL), saturated aqueous NaHCO<sub>3</sub> (30 mL), water (30 mL), and brine (30 mL). The combined organic layers were dried over MgSO<sub>4</sub>, filtered, and the solvent was removed by rotary evaporation (50 °C, 1 atm) to yield (*S*)-(+)-1-phenylethane-1-*d*<sub>1</sub> as a clear colorless oil (750 mg, 7.0 mmol, 64% yield). The NMR data was consistent with previously reported spectra.<sup>2</sup>

<sup>1</sup>H NMR: (400 MHz, CDCl<sub>3</sub>)

δ 7.30 (t, *J* = 7.6 Hz, 2H), 7.25 – 7.16 (m, 3H), 2.72 – 2.58 (m, 1H), 1.25 (d, *J* = 7.6 Hz, 2H).

### III. Cu-catalyzed Transfer Hydrodeuteration Method



**(S)-(+)-[3-[(1,1-dimethylethyl)dimethylsilyloxy]propyl]-benzene-*d*<sub>1</sub> [1a]**. In a N<sub>2</sub> filled glovebox, (*R*)-DTBM-SEGPHOS (52 mg, 0.044 mmol, 0.022 eq.), Cu(OAc)<sub>2</sub> (200 μL, 0.04 mmol, 0.02 eq. of a 0.2 M solution in THF), and THF (1.0 mL) were added to an oven-dried 20-dram vial followed by dropwise addition of DMMS (1 mL, 8.0 mmol, 4.0 eq.). A color change from green/blue to orange was observed while stirring for 15 minutes. In a separate oven-dried 20-dram vial was added [3-[(1,1-dimethylethyl)dimethylsilyloxy]-1-propen-1-yl]-benzene **20** (500 mg, 2.0 mmol, 1.0 eq.), THF (1.0 mL), and ethanol-OD (304 μL, 5.2 mmol, 2.6 eq.). The solution in the 20-dram vial was added dropwise over 20 seconds to the 100 mL

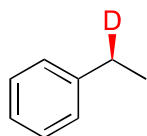
round bottom flask. The total volume of THF was calculated based on having a final reaction concentration of 1 M based on the alkene substrate. The reaction stirred for 16 h at 40 °C in an oil bath. The reaction was filtered through a 2” silica plug with 200 mL Et<sub>2</sub>O into a 500 mL round bottom flask. The resulting crude oil was dry loaded onto a silica gel column and purified by flash column chromatography (400 mL 100% hexanes) to give **1a** as a light tan oil (455 mg, 1.8 mmol, 91% yield).

<sup>1</sup>H NMR: (400 MHz, CDCl<sub>3</sub>)

δ 7.32 – 7.25 (m, 2H), 7.23 – 7.15 (m, 3H), 3.70 – 3.61 (m, 2H), 2.68 (q, *J* = 7.8 Hz, 1H), 1.84 (q, *J* = 7.0 Hz, 2H), 0.92 (d, *J* = 1.0 Hz, 9H), 0.07 (d, *J* = 1.0 Hz, 6H)

Optical Rotation:

$[\alpha]_{546}^{20} = +0.076^{\circ}$



**(S)-(+)-1-Phenylethane-1-*d*<sub>1</sub> [2].** In a N<sub>2</sub> filled glovebox, (*R*)-DTBM-SEGPHOS (149 mg, 0.127 mmol, 0.011 eq.), Cu(OAc)<sub>2</sub> (575 μL, 0.01 mmol, 0.01 eq. of a 0.2 M solution in THF), and THF (5.5 mL) were added to an oven-dried 20-dram vial followed by dropwise addition of PMHS (3.10 mL, 46.0 mmol, 4.0 eq. based on Si-H).<sup>3</sup> A color change from green/blue to orange was observed while stirring for 15 minutes. In a separate oven-dried 100 mL round bottom flask was added vinylbenzene (1.32 mL, 11.5 mmol, 1.0 eq.), THF (6.5 mL), and ethanol-OD (1.80 mL, 29.9 mmol, 2.6 eq.). The solution in the 20-dram vial was added dropwise over 20 seconds to the 100 mL round bottom flask. The total volume of THF was calculated based on having a final reaction concentration of 1M based on the alkene substrate. The reaction stirred for 16 h at 40 °C in an oil bath. The reaction was filtered through a 2” silica plug with 50 mL of pentane by an additional 250 mL into a 500 mL round bottom flask. The crude product was dry loaded by rotary evaporation on an ice bath for 30-45 minutes and purified by flash

column chromatography (300 mL of 100% HPLC hexanes) to yield a clear colorless oil (642 mg, 6.00 mmol, 52% yield).

$^1\text{H NMR}$ : (400 MHz,  $\text{CDCl}_3$ )

$\delta$  7.32 (t,  $J = 7.6$  Hz, 2H), 7.27 – 7.17 (m, 3H), 2.67 (q,  $J = 7.4$  Hz, 1H), 1.27 (d,  $J = 7.6$  Hz, 3H).

$^2\text{H NMR}$ : (61 MHz,  $\text{CHCl}_3$ )

$\delta$  2.70 (s, 1D).

$^{13}\text{C NMR}$ : (101 MHz,  $\text{CDCl}_3$ )

$\delta$  144.24, 128.33, 127.88, 125.61, 28.75 (t,  $J = 19.3$  Hz), 15.57.

ATR-IR ( $\text{cm}^{-1}$ ):

2963, 2926, 2170, 1603, 1495, 1449.

HRMS: ( $\text{EI}^+$ )  $m/z$ :  $[\text{M}]^+$  Calcd for  $\text{C}_8\text{H}_9\text{D}$ , 107.08000; Found 107.08393

Optical Rotation:

$[\alpha]_{365}^{20} = +1.213$

$[\alpha]_{436}^{20} = +0.687$

$[\alpha]_{546}^{20} = +0.371$

$[\alpha]_{589}^{20} = +0.309$

#### IV. Optimization Studies

##### **General procedure for optimization studies of 4-ethyl- 1,1'-biphenyl [3] in Table S1.**

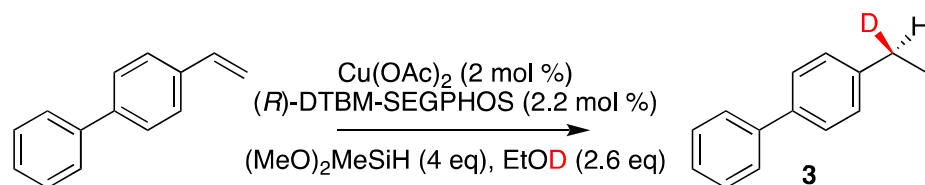
In a  $\text{N}_2$  filled glovebox, (*R*)-DTBM-SEGPHOS (13 mg, 0.011 mmol, 0.022 eq.),  $\text{Cu}(\text{OAc})_2$  (50  $\mu\text{L}$ , 0.01 mmol, 0.02 eq. of a 0.2 M solution in THF), and **solvent** were added to an oven-dried 5-dram vial followed by dropwise addition of DMMS (250  $\mu\text{L}$ , 2.0 mmol, 4.0 eq.). A color change from green/blue to orange was observed while stirring

for 15 minutes. In a separate oven-dried 5-dram was added 4-vinylbiphenyl (90 mg, 0.5 mmol, 1.0 eq.), **solvent**, and EtO-D (76  $\mu$ L, 1.3 mmol, 2.6 eq.). The catalyst solution was added dropwise over 20 seconds to the substrate vial. Reactions run at rt or 40 °C were stirred for 24 h in an oil bath, reactions run at 5 °C were stirred for 48 h. The crude reaction mixture was filtered through a 5'' silica plug with 200 mL hexanes into a 500 mL round bottom flask. The resulting white solid was determined pure by  $^1\text{H}$  NMR to give **3**.

$^1\text{H}$  NMR: (400 MHz,  $\text{CDCl}_3$ )

$\delta$  7.81 – 7.19 (m, 9H), 2.88 – 2.57 (m, 1H), 1.30 (t,  $J = 7.3$  Hz, 3H).

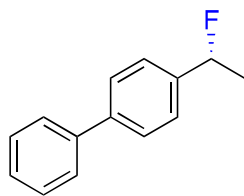
**Table S1: Reaction Optimization**



Entry	Solvent <sup>a</sup>	Concentration <sup>b</sup>	Temp.	% Yield <b>X</b>	% ee <b>X</b>
1	THF	1 M	40 °C	85%	77%
2	THF	1 M	rt	80%	92%
3	THF	1 M	5 °C	98%	96%
4	THF	0.5 M	40 °C	76%	67%
5	1,4-dioxanes	1 M	40 °C	90%	85%
6	4:1 (d:t)	1 M	40 °C	95%	85%
7	1:1 (d:t)	1 M	40 °C	99%	91%
8	1:4 (d:t)	1 M	40 °C	96%	92%
9	MTBE	1 M	40 °C	94%	88%

<sup>a</sup>d:t (1,4-dioxane:THF) <sup>b</sup>Based on 0.5 mmol substrate

## V. Cu-catalyzed Transfer Hydrofluorination



**(R)-4-(1-fluoroethyl)- 1,1'-biphenyl [11].** In a N<sub>2</sub> filled glovebox, (S)-DTBM-SEGPHOS (13 mg, 0.011 mmol, 0.022 eq.), Cu(OAc)<sub>2</sub> (50 μL, 0.005 mmol, 0.01 eq. of a 0.2 M solution in THF), and THF (250 μL) were added to an oven-dried 5-dram vial followed by dropwise addition of DMMS (250 μL, 2.0 mmol, 4.0 eq.). A color change from green/blue to orange was observed while stirring for 15 minutes. In a separate oven-dried 5-dram mL vial was added 4-vinylbiphenyl (90 mg, 0.5 mmol, 1.0 eq.), THF (250 μL), and selectfluor (354 mg, 1.0 mmol, 2.0 eq.). The catalyst solution was added dropwise over 20 seconds to the substrate vial. The total volume of THF was calculated based on having a final reaction concentration of 1 M based on the alkene substrate. The reaction stirred for 24 h at 23 °C in an oil bath. The reaction was filtered through a 2'' silica plug with 50 mL of Et<sub>2</sub>O. The crude product was dry loaded onto SiO<sub>2</sub> by rotary evaporation and purified by flash column chromatography (200 mL hexanes, 300 mL of 2% EtOAc in hexanes) to yield a white solid (33 mg, 0.17 mmol, 33% yield). The NMR data was consistent with previously reported spectra.<sup>4</sup>

<sup>1</sup>H NMR: (400 MHz, CDCl<sub>3</sub>)

δ 7.64-7.61 (m, 4H), 7.49-7.45 (m, 4H), 7.40-7.36 (m, 1H), 5.71 (dq, *J* = 47.6, 6.4 Hz, 1H), 1.71 (dd, *J* = 23.8, 6.4 Hz, 3H).

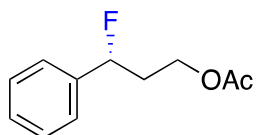
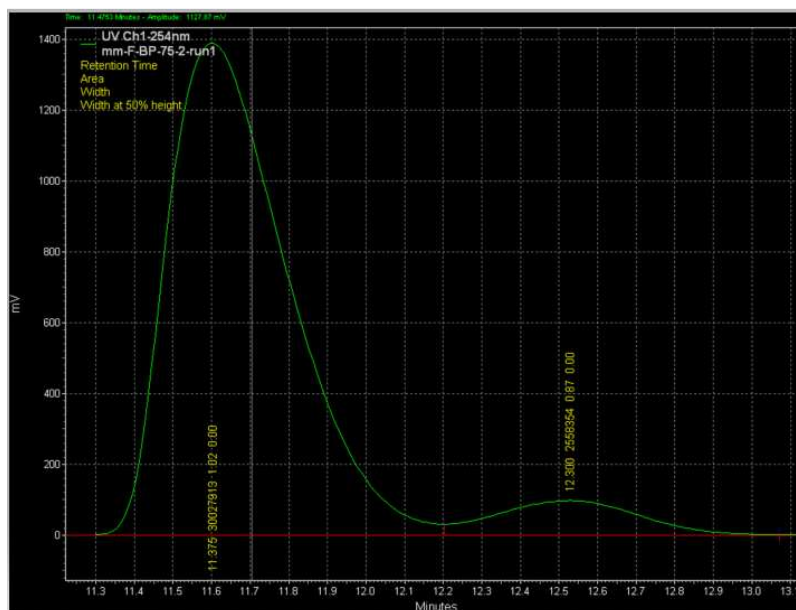
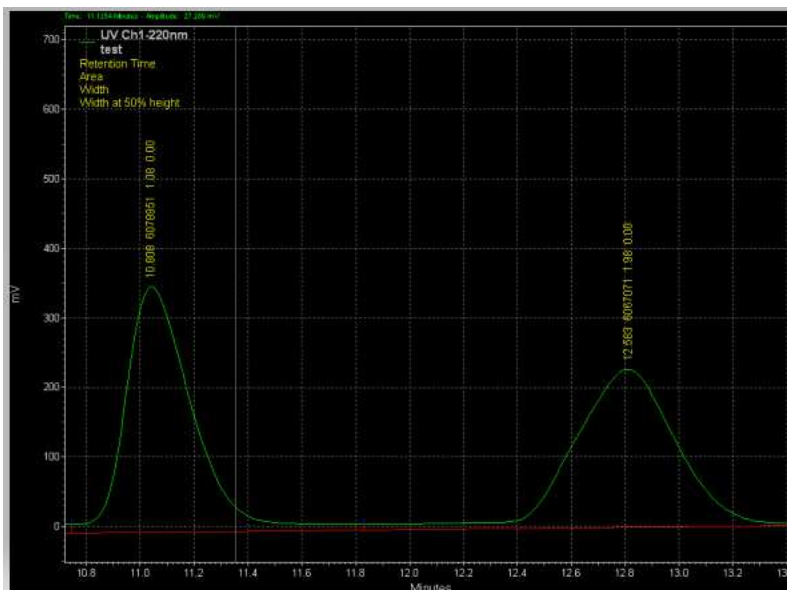
<sup>19</sup>F NMR: (376 MHz, CDCl<sub>3</sub>)

δ -166.6.

HPLC:

[Phenomenex Lux<sup>®</sup> 5 μm Cellulose-3 column, hexanes/*iso*-propanol = 98/2, 1 mL/min, λ = 254, retention time: 11.375 min, (major) and 12.300 min (minor), integration: 30027913 (major) and 2558354 (minor)].





**(R)-  $\gamma$ -Fluoro-, 1-acetate benzenepropanol, [12].** In a  $N_2$  filled glovebox, (S)-DTBM-SEGPHOS (13 mg, 0.011 mmol, 0.022 eq.),  $Cu(OAc)_2$  (50  $\mu$ L, 0.01 mmol, 0.02 eq. of a

0.2 M solution in THF), and THF (250  $\mu$ L) were added to an oven-dried 5-dram vial followed by dropwise addition of DMMS (250  $\mu$ L, 2.0 mmol, 4.0 eq.). A color change from green/blue to orange was observed while stirring for 15 minutes. In a separate oven-dried 5-dram mL vial was added cinnamyl acetate (88 mg, 0.5 mmol, 1.0 eq.), THF (250  $\mu$ L), and selectfluor (364 mg, 1.0 mmol, 2.0 eq.). The catalyst solution was added dropwise over 20 seconds to the substrate vial. The total volume of THF was calculated based on having a final reaction concentration of 1 M based on the alkene substrate. The reaction stirred for 72 h at 23 °C in an oil bath. The reaction was filtered through a 2" silica plug with 50 mL of Et<sub>2</sub>O. The crude product was dry loaded onto SiO<sub>2</sub> by rotary evaporation and purified by flash column chromatography (300 mL of hexanes, 200 mL 2% EtOAc in hexanes) to yield a light tan oil (29 mg, 0.15 mmol, 30% yield). The NMR data was consistent with previously reported spectra.<sup>4</sup> HPLC data has not yet been obtained for **12**.

<sup>1</sup>H NMR: (400 MHz, CDCl<sub>3</sub>)

$\delta$  7.43-7.36 (m, 5H), 5.60 (ddd,  $J$  = 47.7, 8.6, 4.3 Hz, 1H), 4.32-4.19 (m, 2H), 2.37-2.15 (m, 2H), 2.08 (s, 3H).

<sup>19</sup>F NMR: (376 MHz, CDCl<sub>3</sub>)

$\delta$  -177.4

## V. METHODS AND MATERIALS REFERENCES

1. Mosher, H. S.; Elsenbaumer, R.L., Enantiomerically Pure (*R*)-(+)-2-Phenylethanol-2-*d* and -1,1,2-*d*<sub>3</sub>, and (*S*)-(+)-1-Phenylethane-1-*d*, -1,2-*d*<sub>2</sub>, -1,2,2-*d*<sub>3</sub>, and -1,2,2,2-*d*<sub>4</sub>. *J. Org. Chem.* **1979**, *44*, 600-604.
2. Küppers, J.; Rabus, R.; Wilkes, H.; Christoffers, J., Optically Active 1-Deuterio-1-phenylethane – Preparation and Proof of Enantiopurity. *Eur. J. Org. Chem.* **2019**, 2629-2634.
3. Nishikawa, D.; Hirano, K.; Miura, M., Asymmetric Synthesis of  $\alpha$ -Aminoboronic Acid Derivatives by Copper-Catalyzed Enantioselective Hydroamination. *J. Am. Chem. Soc.* **2015**, *137*, 15620-15623.
4. Yin, X.; Chen, B.; Qiu, F.; Wang, X.; Liao, Y.; Wang, M.; Lei, X.; Liao, J., Enantioselective Palladium-Catalyzed Hydrofluorination of Alkenylarenes. *ACS Catalysis* **2020**, *10* (3), 1954-1960.